Meriolins (3-(Pyrimidin-4-yl)-7-azaindoles): Synthesis, Kinase Inhibitory Activity, Cellular Effects, and Structure of a CDK2/Cyclin A/Meriolin Complex †

ARTICLE *in* JOURNAL OF MEDICINAL CHEMISTRY · MARCH 2008

Impact Factor: 5.45 · DOI: 10.1021/jm700940h · Source: PubMed

Meriolins (3-(Pyrimidin-4-yl)-7-azaindoles): Synthesis, Kinase Inhibitory Activity, Cellular Effects, and Structure of a CDK2/Cyclin A/Meriolin Complex†

Aude Echalier,[‡,§] Karima Bettayeb,[⊥,§] Yoan Ferandin,[⊥] Olivier Lozach,[⊥] Monique Clément,[¶] Annie Valette,[×] François Liger,[∞] Bernard Marquet,[∞] Jonathan C. Morris,[#] Jane A. Endicott,[‡] Benoît Joseph,*[,∞] and Laurent Meijer*[,⊥]

Laboratory of Molecular Biophysics and Department of Biochemistry, The Rex Richards Building, University of Oxford, South Parks Road, Oxford, OX1 3QU, U.K., C.N.R.S., Cell Cycle Group & UPS2682, Station Biologique, B.P. 74, 29682 Roscoff Cedex, Bretagne, France, Département de Recherches en Cancérologie, Université de Nantes, Inserm U692, 9 Quai Moncousu, 44093 Nantes Cedex 01, France, LBCMCP, UMR-CNRS 5088, IFR 109, Université Paul Sabatier Bat 4R3B1, 118 Route de Narbonne, 31062 Toulouse Cedex, France, Laboratoire de Chimie Organique 1, Institut de Chimie et Biochimie Moléculaires et Supramoléculaires, UMR-CNRS 5246, Université de Lyon, Université Claude Bernard—Lyon 1, Bâtiment Curien, 43 Boulevard du 11 Novembre 1918, 69622 Villeurbanne Cedex, France, and Department of Chemistry, School of Chemistry and Physics, University of Adelaide, Adelaide SA 5005, Australia

Received July 31, 2007

We report the synthesis and biological characterization of 3-(pyrimidin-4-yl)-7-azaindoles (meriolins), a chemical hybrid between the natural products meridianins and variolins, derived from marine organisms. Meriolins display potent inhibitory activities toward cyclin-dependent kinases (CDKs) and, to a lesser extent, other kinases (GSK-3, DYRK1A). The crystal structures of **1e** (meriolin 5) and variolin B (Bettayeb, K.; Tirado, O. M.; Marionneau-Lambert, S.; Ferandin, Y.; Lozach, O.; Morris, J.; Mateo-Lozano, S.; Drückes, P.; Schächtele, C.; Kubbutat, M.; Liger, F.; Marquet, B.; Joseph, B.; Echalier, A.; Endicott, J.; Notario, V.; Meijer, L. *Cancer Res*. **2007**, *67*, 8325−8334) in complex with CDK2/cyclin A reveal that the two inhibitors are orientated in very different ways inside the ATP-binding pocket of the kinase. A structure−activity relationship provides further insight into the molecular mechanism of action of this family of kinase inhibitors. Meriolins are also potent antiproliferative and proapoptotic agents in cells cultured either as monolayers or in spheroids. Proapoptotic efficacy of meriolins correlates best with their CDK2 and CDK9 inhibitory activity. Meriolins thus constitute a promising class of pharmacological agents to be further evaluated against the numerous human diseases that imply abnormal regulation of CDKs including cancers, neurodegenerative disorders, and polycystic kidney disease.

Introduction

Essentially all physiological processes and most human diseases involve protein phosphorylation. Among the 518 kinases present in man, cyclin-dependent kinases (CDKs[a]) stand out as some of the best studied kinases because of their key functions in cell cycle regulation,[1] neuronal cell physiology,[2] pain signaling,[3] apoptosis,[4] transcription, RNA splicing,[5,6] and insulin secretion.[7] Numerous abnormalities in CDK activity and regulation have been described in cancers.[8] CDK5 is abnormally up-regulated in neurodegenerative disorders such as Alzheimer's,[9] Parkinson's,[10,11] and Nieman-Pick's[12] diseases, in ischemia,[13,14] and in traumatic brain injury.[15] Direct involvement of CDK activities has been demonstrated in viral infections,[16,17] proliferative renal diseases[18–21] including polycystic kidney disease,[22] inflammatory responses,[23] and pain signaling.[3,24] Taken together, these observations in many therapeutic areas constitute strong support for the search for and optimization of selective small molecular weight inhibitors of CDKs. Over 120 pharmacological inhibitors of CDKs have been described (reviews in 25–29). Among these, a few compounds have already reached clinical phase evaluation (Figure 1), mostly against cancer and renal disease. All CDK inhibitors identified so far act by competing with ATP for binding at the catalytic site of their kinase targets.[30] Selectivity studies show that although some kinase inhibitors are rather unselective, many display a definite specificity profile.[31]

Meridianins, a family of 3-(2-aminopyrimidin-4-yl)indoles, were recently identified as kinase inhibitors.[32] Meridianins were first extracted from the Ascidian *Aplidium meridianum*[33] and later chemically synthesized by various groups.[34–36] Meridianins share some structural analogy with another family of marine natural products known as variolins, initially extracted from the Antarctic sponge *Kirkpatrickia variolosa*.[37,38] The synthesis of variolins has been reported recently.[39–43] Variolin B and deoxyvariolin B (PM01218) are cytotoxic to human cancer cell lines.[38,44,45] They are currently under investigation as antitumor drugs by PharmaMar. As this work was in progress, variolin B and deoxyvariolin B were reported to inhibit CDKs.[45]

In this article we report on the synthesis and biological characterization of 3-(pyrimidin-4-yl)-7-azaindoles (meriolins), a chemical hybrid between meridianins and variolins. Meriolins display potent inhibitory activities toward CDKs (especially

† The structures of pT160 CDK2/cyclin A/meriolin 3, pT160 CDK2/cyclin A/meriolin 5, and pT160 CDK2/cyclin A/variolin B have been deposited in the PDB with accession codes 3BHT, 3BHU, and 3BHV, respectively.

* To whom correspondence should be addressed. For B.J. (chemistry): phone, +33 (0)4 72 44 81 35; fax, +33 (0)4 72 44 81 35; e-mail, benoit.joseph@univ-lyon1.fr. For L.M. (biochemistry and cell biology): phone, +33 (0)2 98 29 23 39; fax, +33 (0)2 98 29 25 26; e-mail, meijer@sb-roscoff.fr.

‡ University of Oxford.

§ These authors contributed equally.

⊥ C.N.R.S., Cell Cycle Group & UPS2682.

¶ Université de Nantes.

× Université Paul Sabatier.

∞ Université de Lyon.

University of Adelaide.

[a] Abbreviations: CDK, cyclin-dependent kinase; CK1, casein kinase 1; FCS, fetal calf serum; GSK-3, glycogen synthase kinase-3; LDH, lactate dehydrogenase; MTS, 3-(4,5-dimethylthiazol-2-yl)-5-(3-carboxymethoxyphenyl)-2-(4-sulfophenyl)-2*H*-tetrazolium; PBS, phosphate buffered saline.

10.1021/jm700940h CCC: $40.75
Published on Web 01/31/2008

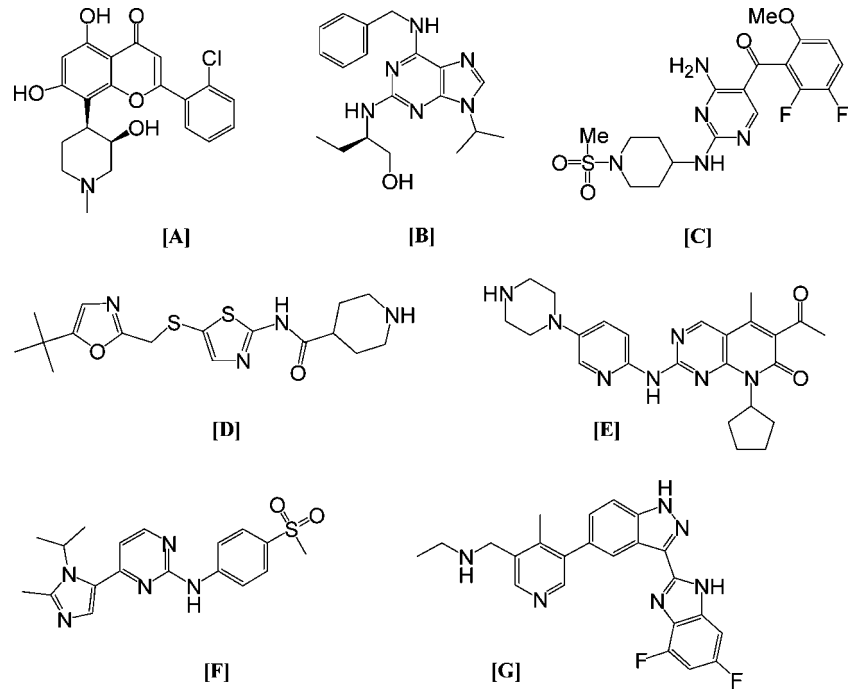

Figure 1. Seven CDK inhibitors currently in clinical trials as anticancer drugs: (A) flavopiridol (Alvocidib) (Sanofi-Aventis);[78] (B) *R*-roscovitine (CYC202, Seliciclib) (Cyclacel Pharmaceuticals);[79,80] (C) R547 (Ro-4584820) (Hoffmann-LaRoche Inc.);[81,82] (D) SNS-032 (BMS-387032) (Bristol-Myers Squibb);[83] (E) PD-0332991 (Pfizer);[84] (F) AZD5438 (AstraZeneca);[85] (G) AG-024322 (Pfizer).[29]

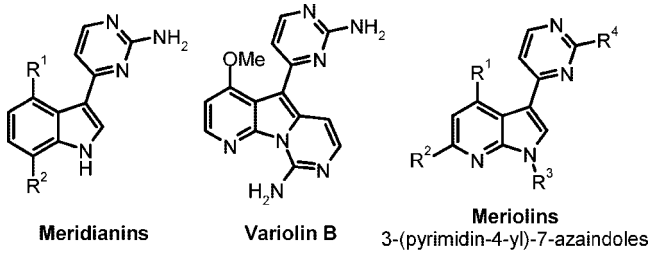

Figure 2. Structure of meriolins and related compounds. Meridianins originate from the Ascidian *Aplidium meridianum*,[33] while variolins were initially extracted from the Antarctic sponge *Kirkpatrickia variolosa*.[37,38]

CDK9) and other kinases (GSK-3, CK1, DYRK1A). Meriolins are also potent antiproliferative and proapoptotic agents in cell cultures. The crystal structures of **1e** (meriolin 5) and variolin B in complex with CDK2/cyclin A reveal that the two inhibitors are orientated in very different ways inside the ATP-binding pocket of the kinase. A structure−activity relationship provides some further insight into the molecular mechanism of action of this family of kinase inhibitors. Proapoptotic efficacy of meriolins correlates best with their CDK2 and CDK9 inhibitory activity.

Results and Discussion

The chemical structure resemblance between the two natural products meridianins and variolin B prompted us to synthesize a hybrid structure, which we named meriolins (Figure 2).

Chemistry. The synthetic approach of meriolins was based on the previous preparation of 3-[(2-amino)pyrimidin-4-yl]-7-azaindole **1** from commercially available 7-azaindole.[46] 4-Chloro-7-azaindole **2a**, 4-methoxy-7-azaindole **2b**, and 6-bromo-7-azaindole **2c** were commercially available. Starting materials **2d**, **2e**, and **2f** were obtained by Mitsunobu reaction between 4-hydroxy-7-azaindole (see Experimental Section)[47] and appropriate alcohols. Acylation of **2a**−**e** in the presence of acetic anhydride and trifluoroacetic acid afforded the derivatives **3a**−**e** (Scheme 1).[48] N-Benzenesulfonylation of **3a**−**e** was readily carried out in the presence of benzenesulfonyl chloride and sodium hydride to give derivatives **4a**−**e**. 3-Acetyl-1-benzenesulfonyl-4-(1-methylethyl)-7-azaindole **4f** was prepared by an

Scheme 1[a]

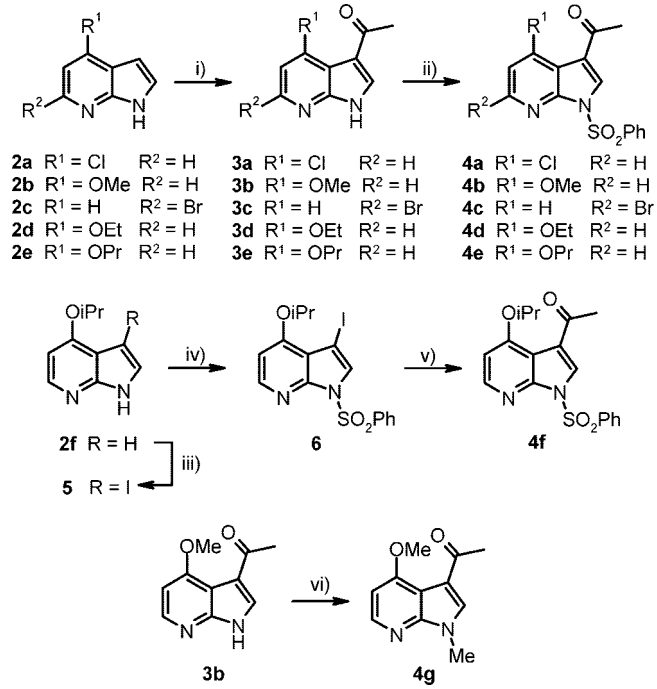

[a] Reagents and conditions: (i) Ac_2O, TFA, reflux, 8 h, **3a** = 85%, **3b** = 55%, **3c** = 99%, **3d** = 84%, **3e** = 80%; (ii) NaH, $PhSO_2Cl$, 0 °C to room temp, 4 h, **4a** = 93%, **4b** = 90%, **4c** = 88%, **4d** = 68%, **4e** = 70%; (iii) I_2, KOH, DMF, room temp, 2.5 h, 82%; (iv) NaH, $PhSO_2Cl$, 0 °C to room temp, 4 h, 68%; (v) (a) *n*-tributyl(1-ethoxyvinyl)stannane, $Pd(PPh_3)_4$, LiCl, DMF, 80 °C, 18 h; (b) 10% HCl, 89%; (vi) Me_2SO_4, K_2CO_3, acetone, reflux, 5.5 h, 81%.

Scheme 2[a]

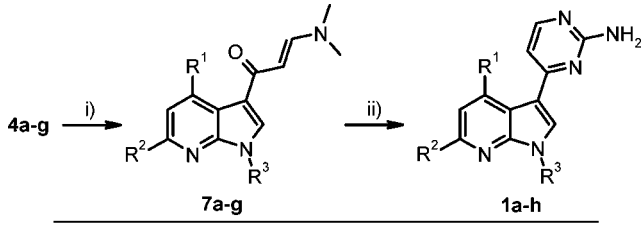

7, **1** - Yield (%)	R^1	R^2	R^3
7a - 60	Cl	H	SO_2Ph
7b - 78	OMe	H	SO_2Ph
7c - 62	H	Br	SO_2Ph
7d - 68	OEt	H	SO_2Ph
7e - 69	OPr	H	SO_2Ph
7f - 69	OiPr	H	SO_2Ph
7g - 82	OMe	H	Me
1a - 51	Cl	H	H
1b - 75	OMe	H	H
1c - 68	H	Br	H
1d - 63	OEt	H	H
1e - 60	OPr	H	H
1f - 60	OiPr	H	H
1g - 92	OMe	H	Me
1h - 31	$O(CH_2)_2OMe$	H	H

[a] Reagents and conditions: (i) DMF-DMA, DMF, 90 °C, 8 h; (ii) guanidine·HCl, K_2CO_3, 2-methoxyethanol, 100–110 °C, 36 h.

alternative way to avoid the O-dealkylation of 7-azaindole **2f** during the first acetylation step in acidic conditions (Scheme 1). Iodination of 4-(1-methylethyl)-7-azaindole **2f** was first realized to give 3-iodo derivative **5**. N-Benzenesulfonation of **5** was then performed to reach **6**. Stille reaction between **6** and tri-*n*-tributyl(1-ethoxyvinyl)stannane afforded the desired derivative **4f**.[49] N-Methylation of compound **3b** was also performed to give derivative **4g**. Reaction of **4a**−**g** with dimethylformamide dimethylacetal in DMF afforded enaminones **7a**−**g** (Scheme 2). Final formation of pyrimidine nucleus occurred by heating **7a**−**g** in the presence of guanidine·HCl and anhydrous K_2CO_3 in 2-methoxyethanol to afford final derivatives **1a**−**g** in fair yields. Under these reaction conditions, compound **7a** gave **1a** (51%) and **1h** (31%) via the displacement of the chlorine atom by the alcohol. O-Demethylation of **1b** and **1g** was done in acidic conditions (48% HBr/AcOH) to reach 4-hydroxy derivatives **8** and **9** in good yields. Derivatives **10** and **11** were prepared from **2b** (Scheme 3). The latter compound was treated with CuCl and formamide to give compound **10** in 26% yield.[50] O-Demethylation of **10** afforded **11** in 92% yield. Compound **12** was prepared in 30% yield by heating **7b** and 2-methyl-2-pseudsothiourea sulfate.[51]

Cocrystallization of Meriolin and Variolin with CDK2/Cyclin A. We report the structure of CDK2/cyclin A in complex with meriolin 5 (compound **1e**) and compare it to that of the structures of complexes of CDK2/cyclin A bound to meriolin 3 (compound **1b**) and to variolin B. CDK2 adopts a fully active conformation upon association with one of its cyclin partners (cyclin A or E) and phosphorylation of Thr160 in the CDK2 activation loop. CDK2 displays a classical protein kinase fold with the N-terminal lobe (composed of a twisted antiparallel β-sheet) linked by a short hinge to the C-terminal domain (which is almost exclusively α-helical).[30]

Scheme 3[a]

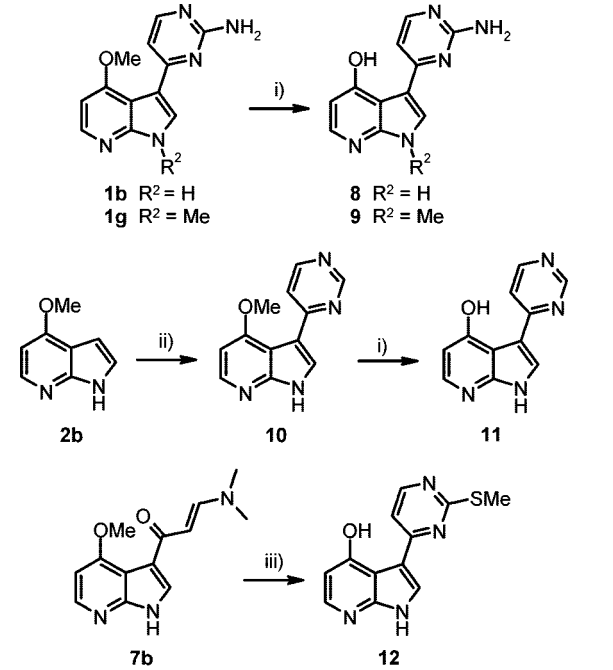

[a] Reagents and conditions: (i) 48% HBr/AcOH, reflux, 2 h, **8** = 90%; **9** = 92%; **11** = 92%; (ii) CuCl, formamide, 170 °C, 18 h, 26%; (iii) 2-methyl-2-thiopseudourea sulfate, K_2CO_3, 2-methoxyethanol, 100–110 °C, 5 days, 30%.

The difference electron density map for the CDK2/cyclin A/meriolin 5 complex after cycles of rigid body refinement showed strong density at the CDK2 ATP binding site. The quality of the data and the resulting electron density maps resulted in the unambiguous positioning of the inhibitor in the electron density map (Figure 3).

Meriolin 5 is bound within the kinase ATP binding cleft, and with the exception of the glycine-rich loop (residues 12–20) that will be described in detail below, the overall conformation of CDK2/cyclin A bound to meriolin 5 is essentially identical to that bound to meriolin 3 (described in ref 66). The binding modes of the two inhibitors are also identical. The pyrrolopyridine central scaffold of meriolins 5 and 3 and the pyrrolopyrimidine system fused to the pyridine ring of variolin B (as described in ref 66) are sandwiched between the two lobes of CDK2. The ring systems pack against the side chain of Leu134 and of Ala31. This is a common feature of many protein kinase inhibitors containing planar ring scaffolds.

As described for ATP and for almost all ATP-competitive kinase inhibitors, the meriolins and variolins also interact with CDK2 via hydrogen bonds with the hinge region of the protein, namely, with the Glu81 main chain carbonyl group and the Leu83 main chain amide nitrogen (Figures 3 and 4). Interestingly, despite sharing a large proportion of their scaffold, meriolin 5 and variolin B interact with the CDK2 hinge via different groups. These interactions occur with the pyrrole-pyridine core of meriolin 5 and through the pyridine-amine ring of variolin B (Figures 3 and 4, respectively). As a result, the two inhibitors explore different regions of the CDK2 ATP site.

The different orientations of the meriolin 5 and variolin B scaffolds result in the meriolin 5 pyrrole ring facing the gatekeeper residue Phe80 (Figure 3). However, in the variolin B structure this ring faces out of the ATP site toward the selectivity surface (Figure 4). It is likely that the pyridine-amine group of variolin B is too bulky to be accommodated in the space facing the gatekeeper, and as a result, the inhibitor is rotated 180° compared to the binding

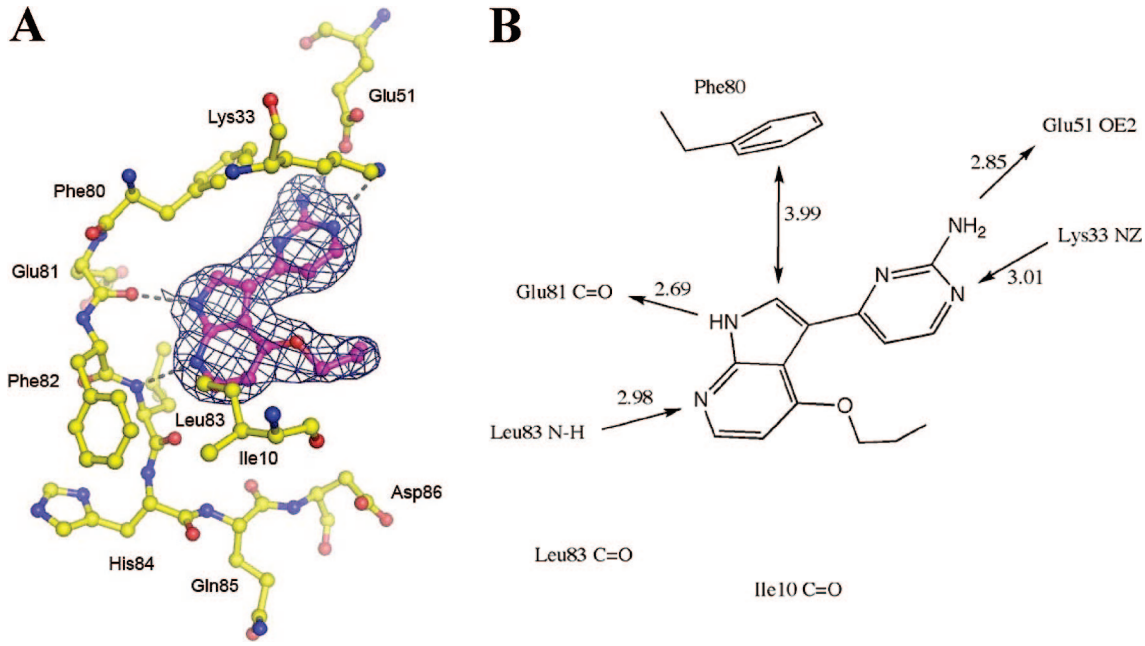

Figure 3. Cocrystal structure of meriolin 5 (**1e**) bound to CDK2/cyclin A. (A) $(2F_o - F_c)\alpha_{calc}$ electron density for meriolin 5 calculated at the end of refinement using map coefficients output from REFMAC with resolution between 20.0 and 2.3 Å. The map is contoured at a level of 0.27 e Å^{-3} corresponding to 1.0 times the rms deviation of the map from its mean value. CDK2 residues surrounding the meriolin 5 molecule are drawn in ball and stick mode. Meriolin 5 carbon atoms are drawn in magenta and those of CDK2 in yellow. Oxygen atoms are colored red, and nitrogen atoms are blue. Dotted lines represent hydrogen bonds. (B) Schematic diagram of the meriolin 5 binding mode. Arrows indicate hydrogen bonds and the distance (Å) between the donor and acceptor atoms.

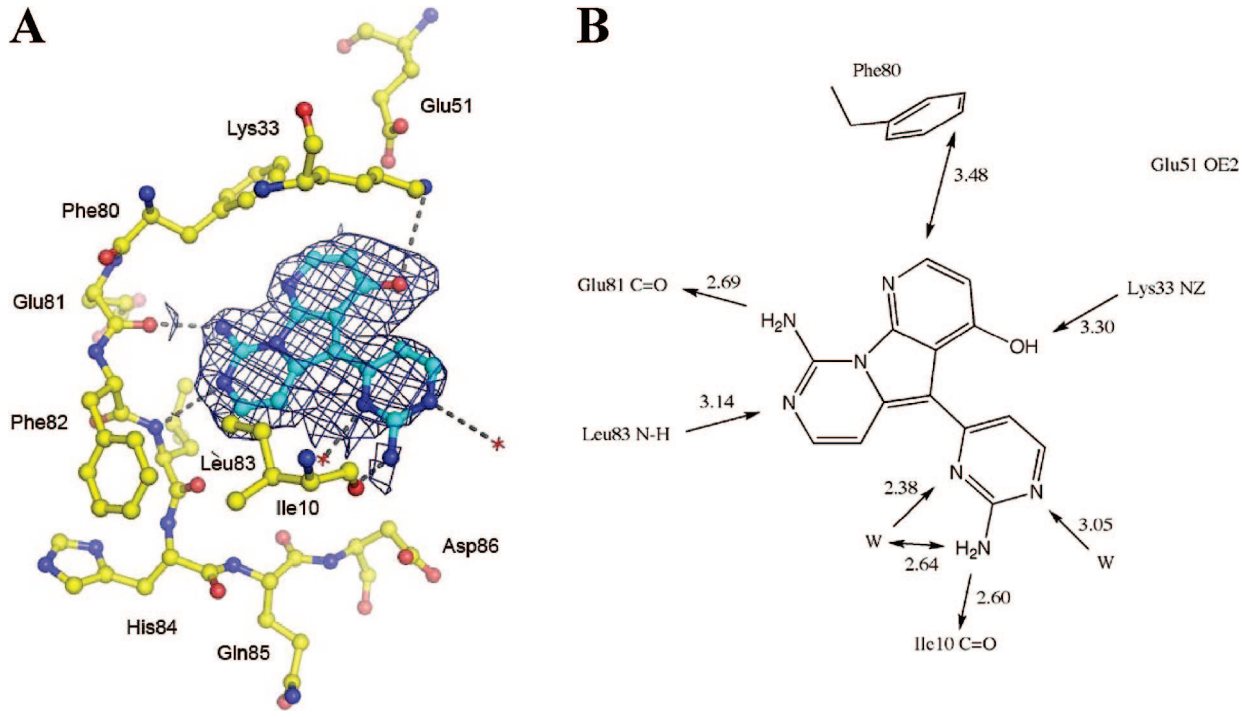

Figure 4. Cocrystal structure of variolin B bound to CDK2/cyclin A. (A) $(2F_o - F_c)\alpha_{calc}$ electron density for variolin B calculated at the end of refinement using map coefficients output from REFMAC with resolution between 20 and 2.1 Å. The map is contoured at a level of 0.27 e Å^{-3} corresponding to 1.0 times the rms deviation of the map from its mean value. CDK2 residues surrounding the variolin B molecule are drawn in ball and stick mode. Variolin B carbon atoms are drawn in cyan, and other color symbols are as in Figure 3. (B) Schematic diagram of the variolin B binding mode. Arrows indicate hydrogen bonds and the distance (Å) between the donor and acceptor atoms.

mode of meriolin 5. Meriolin 5 additionally interacts via its pyrimidine-amine group with the side chains of Glu51 and Lys33 at the back of the ATP cleft (Figure 3), whereas variolin B only interacts with the side chain of Lys33 via the hydroxyl group of its pyridine ring.

The glycine-rich loop is the only CDK2 structural motif that differs between the structures discussed in this report. This loop undergoes rearrangements upon activation and on inhibitor binding, the extent of which is dependent on the ligand bound at the active site.[86–88] It is inherently flexible and upon activation

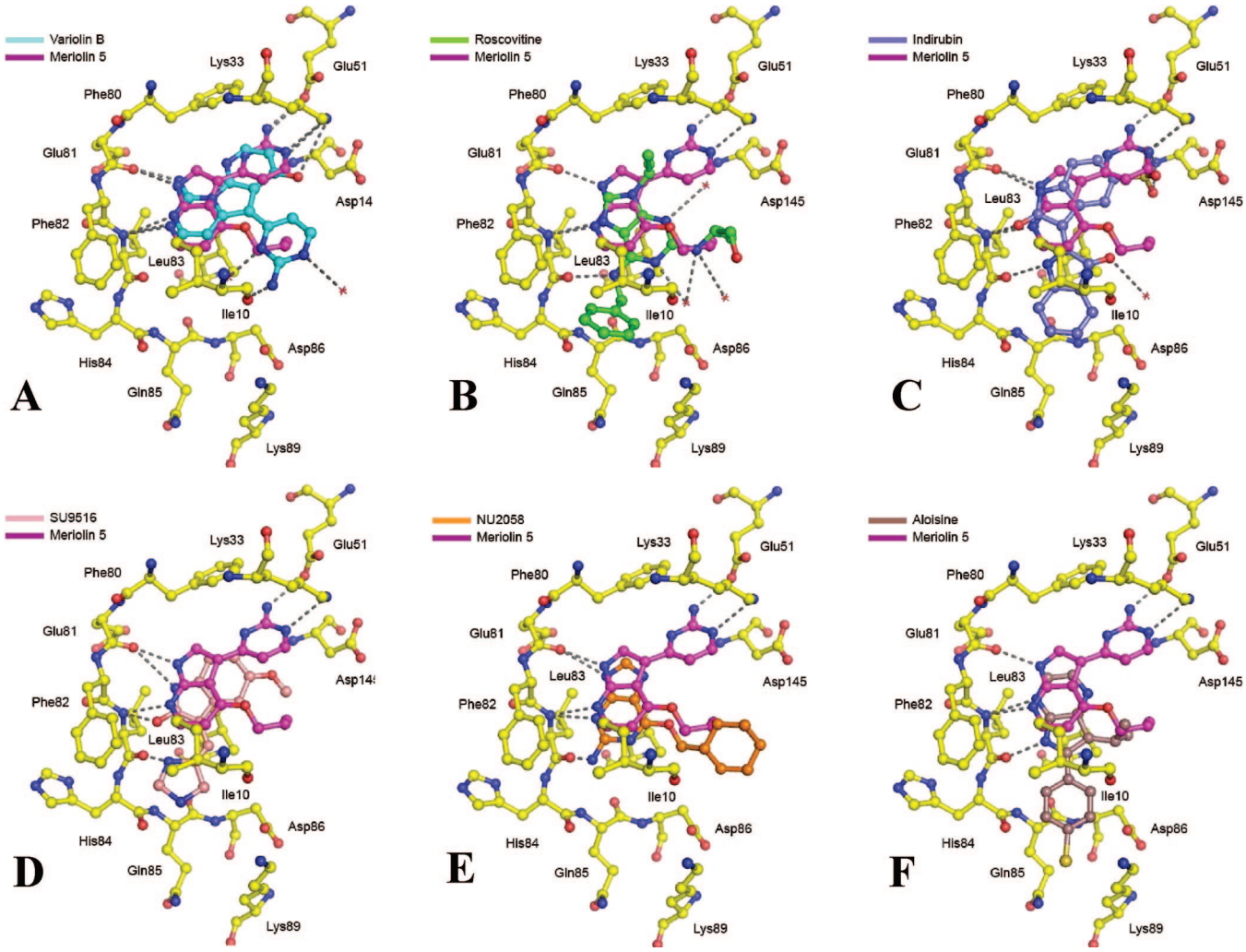

Figure 5. Comparison of the binding modes of meriolin 5 (**1e**) and other CDK inhibitors within the CDK2 ATP-binding pocket. The crystal structure of CDK2/cyclin A in complex with meriolin 5 (PDB code 3BHT) was superimposed on that of CDK2/cyclin A-variolin B (PDB code 3BHV) (A), CDK2/cyclin A-roscovitine (PDB code, in preparation) (B), CDK2/cyclin A-indirubin-3′-oxime-5-sulfonate (PDB code 1E9H) (C), CDK2-SU9516 (PDB code 1PF8) (D), CDK2/cyclin A-NU2058 (PDB 1H1P) (E), CDK2-aloisine A (M. Noble, personal communication) (F). CDK2 residues (taken from the meriolin 5 complex structure) surrounding the inhibitors are drawn in ball and stick mode. Meriolin 5 carbon atoms are drawn in magenta and those of CDK2 in yellow. Dotted lines represent hydrogen bonds, and red stars represent water molecules.

moves away from the active site to expose the ribose binding site to solvent. The loop retains its flexibility in fully activated CDK2, and different orientations have been described in several pThr160-CDK2/cyclin A/ATP-competitive inhibitor complex structures. For example, NU2058 bound to CDK2/cyclin A promotes interactions between the side chains of Tyr15 and Glu51 and between the Thr14 side chain and the Asp145 carboxylate group.[86] The same interactions are observed in one of the two copies of CDK2 within the asymmetric unit of the CDK2/cyclin A/meriolin 5 crystal. However, in the variolin B-bound structure, the glycine-rich loop is located slightly further away from the ATP cleft and is more flexible such that Tyr15 in one copy has weak density and a dual conformation was modeled. The size and the orientation of variolin B in the active site are likely to cause this conformational change. In contrast with the meriolin 5 structure in which the pyrimidine-amine group is located at the back of the ATP cleft, the pyrimidine-amine group in the variolin B structure packs against the glycine-rich loop and bulges slightly out of the cleft (Figure 4). Indeed, this side of variolin B is decorated with water molecules bridging it to the glycine-rich loop. It is anticipated that, despite being numerous, the interactions of variolin B with the CDK2 glycine-rich loop are not very strong because this region of the protein displays signs of flexibility. In contrast, meriolin 5 seems to better stabilize the glycine-rich region. However, even between these two closely related compounds differences in the orientation of Tyr15 can be seen. The molecular basis of these two different conformations is not clear but further outlines the inherent flexibility of this region.

We next compared the CDK2/cyclin A/meriolin 5 structure with other inhibitors that have been cocrystallized with CDK2 (Figure 5), namely, variolin B,[66] roscovitine,[52] indirubin 3′-oxime-5-sulfonate,[53] SU9516,[54] NU2058,[55] and aloisine A.[56] All these inhibitors are ATP-competitive and form at least two hydrogen bonds with the hinge region of CDK2. A third hydrogen bond, with the carbonyl group of Leu83, is observed with roscovitine (Figure 5B), indirubin 3′-oxime-5-sulfonate (Figure 5C), SU9516 (Figure 5D), NU2058 (Figure 5E), and aloisine A (Figure 5F). An appropriate substitution on meriolin might provide this additional hydrogen bond to Leu83 to enhance binding. Among the inhibitors described here, only meriolins 5 and 3, variolin B, and indirubin 3′-oxime-5-sulfonate (through the sulfonate substituent) make a hydrogen bond with the side chain of Lys33 and only the meriolins interact

Table 1. CDK2/Cyclin A (**1b**, Meriolin 3), CDK2/Cyclin A (**1e**, Meriolin 5), and CDK2/Cyclin A (Variolin B) Cocrystal Structures: Statistics of the Data Sets Used and of the Refined Structures

	CDK2/cyclin A (meriolin 3, **1b**)	CDK2/cyclin A (meriolin 5, **1e**)	CDK2/cyclin A (variolin B)
cell dimension (Å)	74.1, 133.8, 147.8	74.1, 134.0, 147.8	74.2, 134.0, 147.9
maximal resolution (Å)	2.00	2.30	2.10
observations	347 777	209 608	345 484
unique reflections, completeness (%)	95 411 (95.5)	65 608 (99.3)	86 384 (99.7)
R_{merge}[a]	0.051	0.087	0.068
mean $I/\sigma(I)$	16.3	11.1	13.1
highest resolution bin (Å)	2.11–2.00	2.42−2.30	2.21–2.10
completeness (%)	77.0	98.3	98.9
(mean I)/(mean $\sigma(I)$)	4.8	3.0	3.8
R_{merge}	0.225	0.439	0.386
resolution range (Å)	20.00–2.00	20.00–2.30	20.00–2.10
R_{conv}[b]	0.181	0.194	0.182
R_{free}[c]	0.220	0.240	0.229
mean protein temperature factors (Å)[b]	8.4	10.4	36.7
mean ligand temperature factors (Å)[b]	2.3	4.2	42.1
PDB code	3BHT	3BHU	3BHV

[a] $R_{merge} = (\sum_h \sum_j I_{h,j} - I^-_h)/(\sum_h \sum_j I_{h,j})$, where $I_{h,j}$ is the intensity of the jth observation of unique reflection h. [b] $R_{conv} = (\sum_h ||F_{o,h}| - |F_{c,h}||)/(\sum_h |F_{o,h}|)$, where $F_{o,h}$ and $F_{c,h}$ are the observed and calculated structure factor amplitudes for reflection h. [c] R_{free} is equivalent to R_{conv} but is calculated using a 5% disjoint set of reflections excluded from the least-squares refinement stages.

Table 2. Effects of Variolin B and **1**, **1a**−**h**, **8**–**12** (Meriolins 1–14) on Seven Protein Kinases[a]

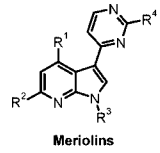

Meriolins

#	Meriolin	R^1	R^2	R^3	R^4
1	1	H	H	H	NH_2
8	2	OH	H	H	NH_2
1b	3	OMe	H	H	NH_2
1d	4	OEt	H	H	NH_2
1e	5	OPr	H	H	NH_2
1f	6	OiPr	H	H	NH_2
1h	7	$O(CH_2)_2OMe$	H	H	NH_2
9	8	OH	H	Me	NH_2
1g	9	OMe	H	Me	NH_2
1a	10	Cl	H	H	NH_2
1c	11	H	Br	H	NH_2
12	12	OMe	H	H	SMe
11	13	OH	H	H	H
10	14	OMe	H	H	H

	compd	CDK1/cyclin B	CDK2/cyclin A	CDK5/p25	CDK9/cyclin T	GSK-3α/β	CK1	DYRK1A
	variolin B	0.06	0.08	0.09	0.026	0.07	0.005	0.08
1	meriolin 1	0.78	0.09	0.51	0.026	0.63	0.2	0.13
8	meriolin 2	0.057	0.018	0.050	0.018	0.40	0.05	0.035
1b	meriolin 3	0.17	0.011	0.17	0.006	0.23	0.2	0.029
1d	meriolin 4	0.01	0.007	0.005	0.007	0.03	0.1	0.032
1e	meriolin 5	0.007	0.003	0.003	0.0056	0.025	0.2	0.037
1f	meriolin 6	0.008	0.0051	0.003	0.0056	0.021	0.14	0.040
1h	meriolin 7	35.0	>10	14.0	5.30	63.0	100.0	>10
9	meriolin 8	1.20	1.8	5.50	1.2	4.60	2.3	1.2
1g	meriolin 9	25.0	>10	73.0	>10	>100	>10	>10
1a	meriolin 10	0.24	0.06	0.23	0.05	2.00	3.0	0.13
1c	meriolin 11	2.20	1.3	0.68	1.00	30.0	1.3	0.3
12	meriolin 12	1.80	2.1	2.30	1.10	7.00	0.6	1.0
11	meriolin 13	0.9	0.7	0.7	0.25	1.8	0.9	0.9
10	meriolin 14	1.3	0.8	1.3	0.22	1.1	0.6	0.23

[a] Variolin B and meriolins were tested at various concentrations in seven kinase assays, as described in the Experimental Section. IC_{50} values were calculated from the dose–response curves and are reported in micromolar.

with the Glu51 side chain. A more detailed comparative analysis of these cocrystal structures is provided in the Supporting Information.

Kinase Inhibitory Activities and Structure−Activity Relationship. All synthesized meriolins 1–14, along with variolin B as a reference, were first tested on seven purified protein kinases, CDK1/cyclin B, CDK2/cyclin A, CDK5/p25, CDK9/cyclin T, GSK-3α/β, CK1δ/ϵ, and DYRK1A (Table 2). Meriolins 1–6 are potent inhibitors of all seven kinases. As previously observed for many CDK inhibitors, meriolins and variolin B are also high to low nanomolar inhibitors of GSK-3β.[57] This albeit limited SAR study, complemented with the crystal structure, provides clear-cut information on the interactions of meriolins with kinases.

Meriolin 5 binds to the CDK2 hinge region via hydrogen bonds involving the two nitrogens within the pyrrolo[2,3-*b*]pyridine ring. These positions are therefore anticipated to tolerate little variation. This is confirmed to be the case for all protein kinases tested in this study by the loss of potency of meriolins upon addition of a methyl group at the position R3 (compare meriolins 2 and 8, and compare meriolins 3 and 9).

Position R_2 on meriolin 5 faces the main chain carbonyl group of Leu83. Addition of a bromide atom at this position (compare meriolins 1 and 11) leads to a drop in inhibitory activity for almost all protein kinases tested, but this effect is particularly pronounced against CDK9 and GSK-3. CDK1, CDK2, and CDK5 are less affected by the bromide addition. This result might reflect a potential difference between the ATP binding sites of the different CDKs that might be exploited to develop more discriminating inhibitors.

Third, the replacement of the amino group by $-SCH_3$ (compare meriolins 12 and 3) or by $-H$ (compare meriolins 13 and 2, and compare meriolins 14 and 3) also leads to a reduction of inhibitory activity. This is likely to result from the loss of a key hydrogen bond between the amine group on the pyrimidine ring with CDK2 Glu51 (Figure 3).

Fourth, we investigated the effects of substitution at position R_1. The effects of the substitutions could be rationalized by reference to the structures of CDK2/cyclin A/meriolin 3 (ref 66) and /meriolin 5 (this study). The inhibitory activity of the meriolins was particularly sensitive to modifications at this position. Increasing the size of aliphatic groups added at R_1 (meriolins 2−6) resulted in an increase in affinity. Groups at R_1 interact with the glycine-rich loop region, and the propyl group of meriolin 5 is observed to pack more extensively against the glycine-rich loop than the smaller meriolin 3 methyl group. The most potent inhibitors in this series were meriolins 5 and 6, which exhibited IC_{50} values in the low nanomolar range for CDKs (Table 2), 20 nM for GSK-3, 40 nM for DYRK1A, and submicromolar values for CK1.

As this work was in progress, 3-(N-substituted 2-aminopyrimidin-4-yl)-7-azaindoles were reported as potent CDK1 inhibitors.[58] These molecules share the central core of meriolins but have bulky substitutions on the pyrimidin-2-ylamine group that would appear to be incompatible with the mode of binding of the meriolins to CDK2. However, an unambiguous assignment of the binding mode must await determination of a CDK2 cocomplex structure with Dr. Huang's molecules.

Cellular Effects of Meriolins. All synthesized meriolins **1**–**14** were next tested for their effect on cell survival of five cell lines: neuroblastoma SH-SY5Y cells, HEK293 cells, glioma GBM cells, multiple myeloma KMS-11, and colorectal adenocarcinoma LS 174T cells (Table 3). Cell survival was estimated 48 h after the addition of each compound using the MTS reduction assay (SH-SY5Y, HEK293, LS 174T) or neutral red (GBM, KMS-11). IC_{50} values were calculated from the dose–response curves. Some meriolins were particularly potent at compromising cell survival. Although an overall correlation was observed between kinase inhibition of the six enzymes with cell death induction, an excellent correlation was observed with inhibition of CDK9 (Tables 2 and 3) with the exception of meriolin 10.

We next tested the effects of all these compounds on the phosphorylation of several CDK substrates in neuroblastoma SH-SY5Y cells (Figure 6). Some meriolins prevented the phosphorylation of retinoblastoma protein (CDK2/CDK4 sites)[59] (Figure 6A), protein phosphatase 1α (CDK1 site)[60] (Figure 6B), and RNA polymerase II (CDK9 site)[61] (Figure 6C). The meriolins that were initially detected as being most active at inhibiting purified kinases (Table 2) and at inducing cell death (Table 3) were also found to be the most active at inhibiting site-specific phosphorylation of CDK substrates in cell culture. In agreement with the extreme sensitivity of CDK9 to several meriolins in vitro, the in vivo phosphorylation of RNA polymerase II on Ser2, its CDK9-specific site, was most sensitive to the same meriolins (Figure 6C).

Table 3. Effects of Variolin B and **1**, **1a**−**h**, **8**–**12** (Meriolins 1–14) on the Survival of Various Cell Lines[a]

	compd	SH-SY5Y	HEK293	GBM	KMS-11	LS 174T
	variolin B	0.24	1.92	0.33 ± 0.12	0.08 ± 0.04	0.88
1	meriolin 1	0.67	2.20	1.38 ± 0.21	1.27 ± 0.27	1.50
8	meriolin 2	0.41	0.96	1.21 ± 0.39	0.60 ± 0.10	1.06
1b	meriolin 3	0.073	0.24	0.14 ± 0.10	0.12 ± 0.02	0.13
1d	meriolin 4	0.081	0.22	0.13 ± 0.09	0.06 ± 0.03	0.10
1e	meriolin 5	0.026	0.085	0.08 ± 0.03	0.04 ± 0.01	0.047
1f	meriolin 6	0.038	0.089	0.08 ± 0.02	0.04 ± 0.02	0.060
1h	meriolin 7	>100	>100	>20	>20	>30
9	meriolin 8	>30	>30	>20	>20	>30
1g	meriolin 9	>30	>30	>20	>20	>30
1a	meriolin 10	1.92	10.8	10.0 ± 5	7.5 ± 3.5	>10
1c	meriolin 11	43	>100	>20	>15	>30
12	meriolin 12	>100	66	>20	>20	>30
11	meriolin 13	28.0	84	>20	>15	23.5
10	meriolin 14	10.2	35.5	10.0 ± 6	10.0 ± 4	10.0

[a] Variolin B and meriolins were tested at various concentrations for their effects on neuroblastoma SH-SY5Y cells, HEK293 cells, glioma GBM cells, myeloma KMS-11, and colorectal adenocarcinoma LS 174T cells. Cell survival was estimated 48 h after the addition of each compound using the MTS reduction assay (SH-SY5Y, HEK293, LS 174T) or neutral red (GBM, KMS-11). IC_{50} values were calculated from the dose–response curves and are reported in micromolar (average ± SE of three independent measurements performed in triplicate).

We next analyzed the level of Mcl-1, a key survival factor frequently expressed in tumor cells (reviews in refs 62 and 63), in SH-SY5Y cells exposed to all the synthesized meriolins (Figure 6D). Several meriolins triggered a complete disappearance of Mcl-1. An excellent correlation was observed with inhibition of CDK9 (Tables 2 and 3) with the exception of meriolin 10.

We also assayed the activity of caspases in SH-SY5Y cells exposed to two concentrations of each meriolin (Figure 7). Results show solid induction of caspase activity by the most potent meriolins as detected in vitro (purified kinases) and in vivo (cell death induction, inhibition of CDK substrate phosphorylation, and induction of Mcl-1).

Finally we tested the effects of a 5 day treatment with meriolin 3 on the proliferation of HCT116, a human colon cancer cell line grown in 3D spheroids, using a method adapted from Del Duca et al.[64] This method allows the preparation of individualized spheroids that are homogeneous in terms of size distribution. Each spheroid was prepared from 500 HCT116 cells. Four days after the beginning of the culture, spheroids were treated with various concentrations of meriolin 3 for a 5 day period. The size of the spheroids was then measured under the microscope and compared to the spheroids' size at the beginning of the treatment (Figure 8A). While the control spheroids reached a 1300 μm diameter, the meriolin 3 treated spheroids only reached a diameter of 720 μm. Meriolin 3 prevented HCT116 cell proliferation in a concentration-dependent manner (Figure 8B), with an IC_{50} value of 0.063 ± 0.015 μM. Spheroid culture shows chemoresistance to a wide range of agents compared to conventional monolayers.[65] Meriolin 3 showed equal or even better activity in HCT116 spheroids than in the respective monolayer cell culture (IC_{50} = 0.94 μM),[66] indicating that this compound has the potential to circumvent multicellular drug resistance and, as such, may show promising activity against solid tumors.

Conclusion

Meriolins represent a hybrid structure between the natural products meridianins and variolins and constitute a potent kinase

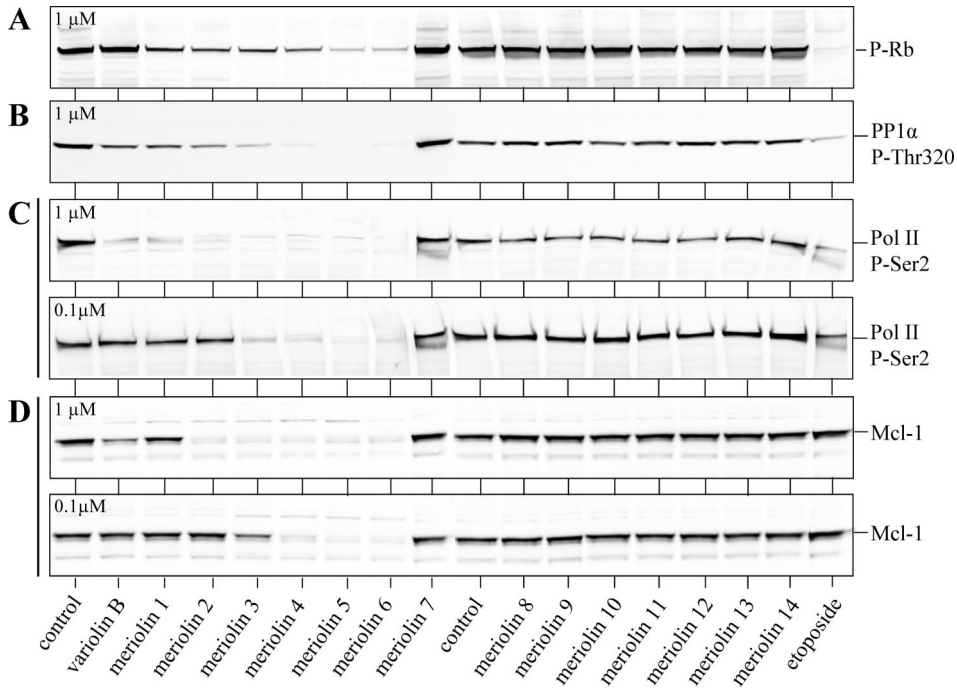

Figure 6. Effects of meriolins 1–14 (**1**, **1a**−**h**, **8**–**12**) and variolin B on the phosphorylation at CDK-specific sites of retinoblastoma protein Rb, protein phosphatase PP1α and RNA polymerase II, and Mcl-1 levels. Cells were exposed for 24 h to variolin B or meriolins 1–14 (0.1 and/or 1 μM final concentration) or vehicle (DMSO). Proteins were then resolved by SDS−PAGE followed by Western blotting with antibodies phospho-Rb (A), phospho-Thr320 PP1α (B), phospho-Ser2 RNA polymerase II (C), and Mcl-1 (D).

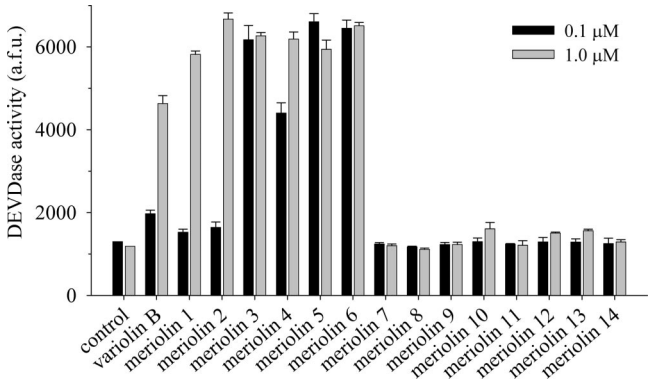

Figure 7. Effects of all meriolins 1–14 (**1**, **1a**−**h**, **8**–**12**), and variolin B on the activity of caspases. Cells were exposed for 24 h to variolin B or meriolins 1–14 (0.1 or 1 μM final concentration) or vehicle (DMSO). DEVDase activity was measured as arbitrary fluorescence units. Every point is the mean ± SE of three independent determinations.

inhibitory scaffold. Their cocrystallization with CDK2/cyclin A and the determination of SARs for a small series of analogues provide some interesting clues in order to understand their molecular mechanism of action and to improve their effects. The strong antiproliferative and proapoptotic effects of meriolins in tumor cells cultured under various conditions (in monolayers, in spheroids, and as xenografts in nude mice[66]) provide a sound rationale for their further optimization and evaluation of their antitumor properties. Meriolins also provide promising pharmacological inhibitors of CDKs involved in noncancer pathologies such as polycystic kidney disease, various neurodegenerative diseases, stroke, inflammation, and some viral infections.

Experimental Section

Chemistry. General Procedures. Commercial reagents (Fluka, Aldrich) were used without purification. Solvents were distilled prior to use. All reactions requiring anhydrous conditions were conducted in a flame-dried apparatus. Melting points were determined using a Büchi capillary instrument and are uncorrected. IR spectra were recorded on a Perkin-Elmer 681 infrared spectrophotometer. ^{1}H NMR and ^{13}C spectra were recorded on a Bruker Avance 300 or 500 MHz spectrometer. Chemical shifts are reported in ppm (δ) relative to tetramethylsilane as an internal standard. Mass spectra were recorded with a Perkin-Elmer SCIEX API spectrometer. Elemental analyses were performed on a Thermoquest Flash 1112 series EA analyzer. Thin layer chromatography (TLC) analyses were conducted on aluminum sheets silica gel, Merck 60F_{254}. The spots were visualized using an ultraviolet light. Flash chromatography was carried out on silica gel 60 (40–63 μm, Merck) using the indicated solvents. The light petroleum ether refers to the fraction boiling at 40–60 °C. Compounds **2a**−**c** were commercially available. 4-Hydroxy-7-azaindole has been prepared according to the previously reported method.[47]

Variolin B. Variolin B was synthesized in eight steps as described previously.[43] The trifluoroacetate salt was neutralized by sonication with concentrated aqueous NH_3/MeOH to give the free base. Concentration in vacuo (35 °C, 0.03 mm/Hg to remove ammonium trifluoroacetate) gave variolin B as a brown-orange solid. Mp 320 °C (dec) (lit.[37] 45 °C, dec). IR (KBr): ν 3085, 1670, 1572, 1477, 1458, 1298 cm^{-1}. ^{1}H NMR (500 MHz, DMSO- d_6): δ 6.81 (d, 1H, J = 5.6 Hz, H-3), 6.97 (s, 2H, NH2), 7.14 (d, 1H, J = 5.6 Hz, H-5′), 7.23 (d, 1H, J = 6.7 Hz, H-6), 7.63 (d, 1H, J = 6.7 Hz, H-7), 8.17 (d, 1H, J = 5.6 Hz, H-2), 8.27 (d, 1H, J = 5.6 Hz, H-6′), 8.45 (broad s, 1H, NH), 9.79 (broad s, 1H, NH), 16.05 (s, 1H, OH). ^{13}C NMR (75 MHz, DMSO- d_6): δ 99.6 (C-5), 100.3 (C-6), 106.0 (C-5′), 107.5 (C-3), 111.2 (C-4a), 137.1 (C-5a), 143.1 (C-2), 144.6 (C-7), 144.9 (C-10a), 150.3 (C-9), 158.3 (C-4′), 159.8 (C-4), 160.0 (C-6′), 161.4 (C-2′). HRMS (ES): calcd for $C_{14}H_{12}N_7O$ (MH^+) 294.1103, found 294.1096.

Deoxyvariolin B. This material was prepared using the synthesis described by Morris and co-workers[43] and afforded deoxyvariolin B as a yellow microcrystalline solid. Mp 220–240 °C (dec) (lit.[41] 160–162 °C). IR (KBr): ν 3304, 3142–2849 (series of weak bands), 1647, 1574, 1514, 1472, 1456, 1269 cm^{-1}. ^{1}H NMR (500 MHz, DMSO-d_6): δ 6.51 (s, 2H, NH_2), 7.05 (d, 1H, J = 5.4 Hz, H-5′),

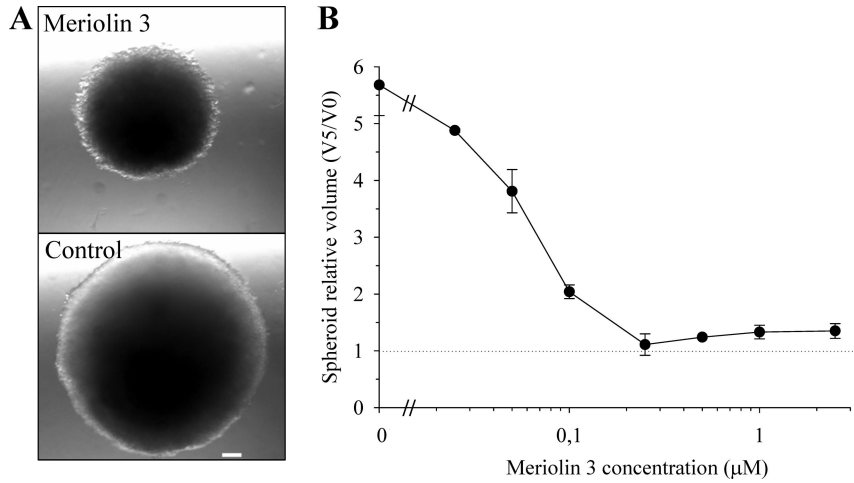

Figure 8. Effects of meriolin 3 (**1b**) on the survival of HCT116 cells grown in spheroids. After 4 days of culture in spheroids, HCT116 cells were exposed to various concentrations of meriolin 3 for 5 days. (A) Photograph of control and meriolin 3 (1 μM) treated spheroids (scale, 100 μm). (B) Spheroid volumes were estimated and compared to those of the initial day spheroid volume. A ratio of 1 (dashed line) indicates complete inhibition of cell growth.

7.57 (dd, 1H, J = 4.8, 8.2 Hz, H-3), 7.62 (d, 1H, J = 6.3 Hz, H-7), 7.67 (d, 1H, J = 6.3 Hz, H-6), 8.22 (d, 1H, J = 5.4 Hz, H-6′), 8.44 (dd, 1H, J = 1.5, 4.8 Hz, H-2), 8.50 (broad s, 1H, NH), 8.90 (dd, 1H, J = 1.5, 8.2 Hz, H-4), 9.40 (broad s, 1H, 9-NH). ^{13}C NMR (75 MHz, DMSO-d_6): δ 99.6 (C-5), 101.9 (C-6), 107.1 (C-5′), 121.0 (C-3), 121.7 (C-4a), 129.4 (C-4), 138.3 (C-5a), 140.3 (C-2), 143.0 (C-10a), 144.0 (C-7), 149.9 (C-9), 158.2 (C-6′), 161.6 (C-4′), 163.6 (C-2′). MS (EI): m/z (rel intensity) 277 (100), 236 (54). HRMS (EI): **calcd for $C_{14}H_{11}N_7$ (M^+) 277.1076, found 277.1072.

3-[(2-Amino)pyrimidin-4-yl]-1 *H*-pyrrolo[2,3-*b*]pyridine (1). Meriolin 1. This compound was prepared using the synthesis described by Fresneda and Molina.[46] Mp >210 °C (MeOH). ^{1}H NMR data (300 MHz, DMSO-d_6) were identical to those described previously.[46]

4-Ethoxy-1*H*-pyrrolo[2,3-*b*]pyridine (2d). Under N_2 atmosphere, diethyl azodicarboxylate (520 μL, 3.3 mmol) was added dropwise to a solution of triphenylphosphine (1.04 g, 3.96 mmol) in dry THF (13 mL). This mixture was added to a solution of 4-hydroxy-7-azaindole (222 mg, 1.65 mmol) and EtOH (115 μL, 1.98 mmol) in dry THF (41 mL). The final mixture was stirred for 2 h at room temperature. The solvent was evaporated. The crude residue was purified by column chromatography (CH_2Cl_2/MeOH, 98:2) to give **2d** (214 mg, 80%). Mp 176–178 °C (Et_2O). ^{1}H NMR (300 MHz, $CDCl_3$): δ 1.52 (t, 3H, J = 7.1 Hz, CH_3), 4.26 (q, 2H, J = 7.1 Hz, CH_2), 6.53 (d, 1H, J = 5.6 Hz, H-5), 6.59 (broad s, 1H, H-3), 7.18 (broad s, 1H, H-2), 8.18 (d, 1H, J = 5.6 Hz, H-6), 9.64 (broad s, 1H, NH). MS (IS): m/z 163 ($M + H^+$). Anal. ($C_9H_{10}N_2O$) C, H, N.

4-Propoxy-1*H*-pyrrolo[2,3-*b*]pyridine (2e). According to the same procedure, compound **2e** was prepared in 78% yield from 4-hydroxy-7-azaindole and PrOH. Mp 189–191 °C (Et_2O). ^{1}H NMR (300 MHz, $CDCl_3$): δ 1.10 (t, 3H, J = 7.4 Hz, CH_3), 1.88–1.99 (m, 2H, CH_2), 4.20 (t, 2H, J = 6.6 Hz, CH_2), 6.59 (d, 1H, J = 5.8 Hz, H-5), 6.63 (d, 1H, J = 3.6 Hz, H-3), 7.21 (d, 1H, J = 3.6 Hz, H-2), 8.15 (d, 1H, J = 5.8 Hz, H-6), 10.34 (broad s, 1H, NH). MS (IS): m/z 177 ($M + H^+$). Anal. ($C_{10}H_{12}N_2O$) C, H, N.

4-(1-Methylethoxy)-1*H*-pyrrolo[2,3-*b*]pyridine (2f). According to the same procedure, compound **2f** was prepared in 76% yield from 4-hydroxy-7-azaindole and *i*-PrOH. Mp 182–184 °C (Et_2O). ^{1}H NMR (300 MHz, $CDCl_3$): δ 1.44 (d, 6H, J = 6.0 Hz, 2 CH_3), 4.82 (hept, 1H, J = 6.0 Hz, CH), 6.52 (d, 1H, J = 5.7 Hz, H-5), 6.57 (d, 1H, J = 3.6 Hz, H-3), 7.19 (d, 1H, J = 3.6 Hz, H-2), 8.17 (d, 1H, J = 5.7 Hz, H-6), 10.70 (broad s, 1H, NH). MS (IS): m/z 177 ($M + H^+$). Anal. ($C_{10}H_{12}N_2O$) C, H, N.

3-Acetyl-4-chloro-1*H*-pyrrolo[2,3-*b*]pyridine (3a). A solution of acetic anhydride (0.13 mL, 1.8 mmol), 4-chloro-7-azaindole **2a** (90 mg, 0.59 mmol), and trifluoroacetic acid (5 mL) was heated at reflux for 8 h. After the mixture was cooled, saturated aqueous Na_2CO_3 was added to neutralize the medium (pH 7–8). After addition of EtOAc, stirring, and decantation, phases were separated. The organic phase was dried over $MgSO_4$ and evaporated. The crude residue was purified by column chromatography (EtOAc) to give **3a** (98 mg, 85%). Mp >210 °C (MeOH). IR (KBr): ν 3196, 3088, 3012, 2872, 1656, 1565, 1455, 1391, 1289, 817 cm^{-1}. ^{1}H NMR (300 MHz, $CDCl_3$): δ 2.63 (s, 3H, CH_3), 7.41 (d, 1H, J = 5.6 Hz, H-5), 8.12 (s, 1H, H-2), 8.27 (d, 1H, J = 5.6 Hz, H-6). MS (IS): m/z 195 ($M + H^+$). Anal. ($C_9H_7ClN_2O$) C, H, N.

3-Acetyl-4-methoxy-1*H*-pyrrolo[2,3-*b*]pyridine (3b). According to the same procedure, compound **3b** was prepared in 55% yield from 4-methoxy-7-azaindole **2b**. Mp >210 °C (MeOH). IR (KBr): ν 3198, 3122, 2841, 1640, 1583, 1463, 1400, 1311, 1100, 848 cm^{-1}. ^{1}H NMR (300 MHz, DMSO-d_6): δ 2.50 (s, 3H, CH_3), 3.92 (s, 3H, CH_3), 6.79 (d, 1H, J = 5.6 Hz, H-5), 8.11 (s, 1H, H-2), 8.17 (d, 1H, J = 5.6 Hz, H-6), 12.36 (broad s, 1H, NH). MS (IS): m/z 191 ($M + H^+$). Anal. ($C_{10}H_{10}N_2O_2$) C, H, N.

3-Acetyl-6-bromo-1*H*-pyrrolo[2,3-*b*]pyridine (3c). According to the same procedure, compound **3c** was prepared in 99% yield from 6-bromo-7-azaindole **2c**. Mp >210 °C (MeOH). IR (KBr): ν 3122, 3035, 2985, 2893, 1651, 1573, 1512, 1418, 1313, 1275, 1102, 943, 918, 818 cm^{-1}. ^{1}H NMR (300 MHz, DMSO-d_6): δ 2.46 (s, 3H, CH_3), 7.42 (d, 1H, J = 8.2 Hz, H-5), 8.38 (d, 1H, J = 8.2 Hz, H-4) 8.49 (d, 1H, J = 3.0 Hz, H-2), 12.68 (broad s, 1H, NH). MS (IS): m/z 241 (^{81}Br, $M + H^+$), 239 (^{79}Br, $M + H^+$). Anal. ($C_9H_7BrN_2O$) C, H, N.

3-Acetyl-4-ethoxy-1*H*-pyrrolo[2,3-*b*]pyridine (3d). According to the same procedure, compound **3d** was prepared in 84% yield from 4-ethoxy-7-azaindole **2d**. Mp >210 °C (MeOH). IR (KBr): ν 3198, 3119, 2837, 1643, 1580, 1463, 1309, 1086, 844 cm^{-1}. ^{1}H NMR (300 MHz, DMSO-d_6): δ 1.43 (t, 3H, J = 7.2 Hz, CH_3), 2.54 (s, 3H, CH_3), 4.22 (q, 2H, J = 7.2 Hz, CH_2), 6.78 (d, 1H, J = 5.7 Hz, H-5), 8.04 (s, 1H, H-2), 8.14 (d, 1H, J = 5.7 Hz, H-6), 12.33 (broad s, 1H, NH). MS (IS): m/z 205 ($M + H^+$). Anal. ($C_{11}H_{12}N_2O_2$) C, H, N.

3-Acetyl-4-propoxy-1*H*-pyrrolo[2,3-*b*]pyridine (3e). According to the same procedure, compound **3e** was prepared in 80% yield from 4-propoxy-7-azaindole **2e**. Mp >210 °C (MeOH). IR (KBr): ν 3198, 3124, 2879, 1640, 1583, 1464, 1401, 1292, 1091, 852 cm^{-1}. ^{1}H NMR (300 MHz, DMSO-d_6): δ 1.07 (t, 3H, J = 7.3 Hz, CH_3), 1.77–1.88 (m, 2H, CH_2), 2.53 (s, 3H, CH_3), 4.11 (t, 2H, J = 6.3 Hz, CH_2), 6.78 (d, 1H, J = 5.6 Hz, H-5), 8.08 (s, 1H, H-2), 8.14 (d, 1H, J = 5.6 Hz, H-6), 12.32 (broad s, 1H, NH). MS (IS): m/z 219 ($M + H^+$). Anal. ($C_{12}H_{14}N_2O_2$) C, H, N.

3-Acetyl-1-benzenesulfonyl-4-chloro-1*H*-pyrrolo[2,3-*b*]pyridine (4a). At 0 °C, sodium hydride (26 mg, 0.64 mmol, 60% in oil) was added portionwise to a solution of **3a** (125 mg, 0.64 mmol) in dry THF (20 mL). The solution was stirred for 45 min at 0 °C, and a solution of benzenesulfonyl chloride (0.11 mL, 0.83 mmol) was added to the reaction mixture. The final solution was stirred at room temperature for 4 h. Addition of water was performed at 0 °C, and then solvent was removed. The residue was partitioned between H_2O and EtOAc (50 mL, 1:1) and extracted. The organic phase was dried over $MgSO_4$ and evaporated. The crude solid was purified by column chromatography (petroleum ether/EtOAc, 8:2) to give **4a** (200 mg, 93%). Mp 160–162 °C (CH_2Cl_2/pentane). IR (KBr): ν 3152, 3020, 2943, 1686, 1382, 1199, 1185, 1092, 995, 746 cm^{-1}. ^1H NMR (300 MHz, $CDCl_3$): δ 2.63 (s, 3H, CH_3), 7.30 (d, 1H, $J = 5.2$ Hz, H-5), 7.54 (broad t, 2H, $J = 7.4$ Hz, H_{arom}), 7.66 (broad t, 1H, $J = 7.4$ Hz, H_{arom}), 8.25 (broad d, 2H, $J = 7.4$ Hz, H_{arom}), 8.32 (d, 1H, $J = 5.2$ Hz, H-6), 8.34 (s, 1H, H-2). MS (IS): *m/z* 335 ($M + H^+$). Anal. ($C_{15}H_{11}ClN_2O_3S$) C, H, N.

3-Acetyl-1-benzenesulfonyl-4-methoxy-1*H*-pyrrolo[2,3-*b*]pyridine (4b). According to the same procedure, compound **4b** was prepared in 90% yield from **3b**. Mp 156–158 °C (CH_2Cl_2/pentane). IR (KBr): ν 3149, 3015, 2943, 1662, 1574, 1511, 1374, 1293, 1196, 1177, 1111, 750 cm^{-1}. ^1H NMR (300 MHz, $CDCl_3$): δ 2.63 (s, 3H, CH_3), 3.98 (s, 3H, CH_3), 6.73 (d, 1H, $J = 5.6$ Hz, H-5), 7.51 (broad t, 2H, $J = 7.4$ Hz, H_{arom}), 7.62 (broad t, 1H, $J = 7.4$ Hz, H_{arom}), 8.21 (s, 1H, H_{arom}), 8.24 (broad d, 2H, $J = 7.4$ Hz, H_{arom}), 8.34 (d, 1H, $J = 5.7$ Hz, H-6). MS (IS): *m/z* 331 ($M + H^+$). Anal. ($C_{16}H_{14}N_2O_4S$) C, H, N.

3-Acetyl-1-benzenesulfonyl-6-bromo-1*H*-pyrrolo[2,3-*b*]pyridine (4c). According to the same procedure, compound **4c** was prepared in 88% yield from **3c**. Mp 172–174 °C (CH_2Cl_2/pentane). IR (KBr): ν 3141, 3087, 1673, 1585, 1529, 1440, 1387, 1207, 1183, 1098, 1087, 974, 929, 758 cm^{-1}. ^1H NMR (300 MHz, $CDCl_3$): δ 2.56 (s, 3H, CH_3), 7.44 (d, 1H, $J = 8.3$ Hz, H-5), 7.58 (broad t, 2H, $J = 7.9$ Hz, H_{arom}), 7.68 (broad t, 1H, $J = 7.9$ Hz, H_{arom}), 8.29 (s, 1H, H_{arom}), 8.31 (broad d, 2H, $J = 7.9$ Hz, H_{arom}), 8.42 (d, 1H, $J = 8.3$ Hz, H-4). MS (IS): *m/z* 381 (^{81}Br, $M + H^+$), 379 (^{79}Br, $M + H^+$). Anal. ($C_{15}H_{11}BrN_2O_3S$) C, H, N.

3-Acetyl-1-benzenesulfonyl-4-ethoxy-1*H*-pyrrolo[2,3-*b*]pyridine (4d). According to the same procedure, compound **4d** was prepared in 68% yield from **3d**. Mp 151–153 °C (CH_2Cl_2/pentane). IR (KBr): ν 3154, 3062, 2981, 1660, 1571, 1508, 1376, 1291, 1197, 1179, 1102, 751 cm^{-1}. ^1H NMR (300 MHz, $CDCl_3$): δ 1.52 (t, 3H, $J = 7.2$ Hz, CH_3), 2.65 (s, 3H, CH_3), 4.21 (q, 2H, $J = 7.2$ Hz, CH_2), 6.70 (d, 1H, $J = 5.7$ Hz, H-5), 7.51 (broad t, 2H, $J = 7.4$ Hz, H_{arom}), 7.61 (broad t, 1H, $J = 7.4$ Hz, H_{arom}), 8.20 (s, 1H, H-2), 8.23 (broad d, 2H, $J = 7.4$ Hz, H_{arom}), 8.31 (d, 1H, $J = 5.7$ Hz, H-6). MS (IS): *m/z* 345 ($M + H^+$). Anal. ($C_{17}H_{16}N_2O_4S$) C, H, N.

3-Acetyl-1-benzenesulfonyl-4-propoxy-1*H*-pyrrolo[2,3-*b*]pyridine (4e). According to the same procedure, compound **4e** was prepared in 70% yield from **3e**. Mp 119–121 °C (CH_2Cl_2/pentane). IR (KBr): ν 3137, 2967, 1676, 1583, 1520, 1496, 1374, 1301, 1189, 1171, 1115, 748 cm^{-1}. ^1H NMR (300 MHz, $CDCl_3$): δ 1.09 (t, 3H, $J = 7.3$ Hz, CH_3), 1.87–1.96 (m, 2H, CH_2), 2.64 (s, 3H, CH_3), 4.09 (t, 2H, $J = 6.6$ Hz, CH_2), 6.70 (d, 1H, $J = 5.7$ Hz, H-5), 7.51 (broad t, 2H, $J = 7.4$ Hz, H_{arom}), 7.61 (broad t, 1H, $J = 7.4$ Hz, H_{arom}), 8.19 (s, 1H, H-2), 8.23 (broad d, 2H, $J = 7.4$ Hz, H_{arom}), 8.31 (d, 1H, $J = 5.7$ Hz, H-6). MS (IS): *m/z* 359 ($M + H^+$) Anal. ($C_{18}H_{18}N_2O_4S$) C, H, N.

3-Iodo-4-(1-methylethoxy)-1*H*-pyrrolo[2,3-*b*]pyridine (5). At room temperature and under an inert atmosphere, a solution of iodine (74 mg, 0.29 mmol) in dry DMF (0.5 mL) was added dropwise to a solution of 4-(1-methylethoxy)-1*H*-pyrrolo[2,3-*b*]pyridine **2f** (50 mg, 0.28 mmol) and potassium hydroxide (88 mg, 1.56 mmol) in dry DMF (0.5 mL). The solution was stirred for 2.5 h at room temperature. The solvent was evaporated, and the crude residue was taken up in water. The suspension obtained was filtered to afford **5** (70 mg, 82%). Mp 181–183 °C (MeOH). IR (KBr): ν 3198, 3116, 2977, 1586, 1509, 1316, 1107, 922, 802 cm^{-1}. ^1H NMR (300 MHz, $CDCl_3$): δ 1.49 (d, 6H, $J = 6.0$ Hz, CH_3), 4.80 (hept, 1H, $J = 6.0$ Hz, CH), 6.55 (d, 1H, $J = 5.8$ Hz, H-5), 7.26 (s, 1H, H-2) 8.14 (d, 1H, $J = 5.8$ Hz, H-6). MS (IS): *m/z* 303 ($M + H^+$). Anal. ($C_{10}H_{11}IN_2O$) C, H, N.

1-Benzenesulfonyl-3-iodo-4-(1-methylethoxy)-1*H*-pyrrolo[2,3-*b*]pyridine (6). Following the procedure described for the preparation of **4a**, compound **6** was obtained in 68% yield from **5**. Mp 151–153 °C (CH_2Cl_2/pentane). IR (KBr): ν 3137, 2979, 1588, 1572, 1487, 1372, 1293, 1189, 1172, 1114, 819, 740 cm^{-1}. ^1H NMR (300 MHz, $CDCl_3$): δ 1.42 (d, 6H, $J = 6.2$ Hz, CH_3), 4.71 (hept, 1H, $J = 6.2$ Hz, CH), 6.59 (d, 1H, $J = 5.7$ Hz, H-5), 7.48 (broad t, 2H, $J = 7.9$ Hz, H_{arom}), 7.58 (broad t, 1H, $J = 7.9$ Hz, H_{arom}), 7.69 (s, 1H, H-2), 8.17 (broad d, 2H, $J = 7.9$ Hz, H_{arom}), 8.27 (d, 1H, $J = 5.7$ Hz, H-6). MS (IS): *m/z* 443 ($M + H^+$). Anal. ($C_{16}H_{15}IN_2O_3S$) C, H, N.

3-Acetyl-1-(1-benzenesulfonyl)-4-(1-methylethoxy)-1*H*-pyrrolo[2,3-*b*]pyridine (4f). To a stirred mixture of **6** (67 mg, 0.15 mmol), freshly prepared $Pd(PPh_3)_4$ (18 mg, 0.015 mmol), and LiCl (16 mg, 0.38 mmol) in dry DMF (3 mL) was added *n*-tributyl(1-ethoxyvinyl)stannane (77 μL, 0.23 mmol). The solution was stirred at 80 °C for 18 h. After the mixture was cooled, 5% HCl solution (10 mL) was added and the solution was stirred for 20 min at room temperature. The solvent was evaporated in vacuo. The residue was partitioned between saturated aqueous Na_2CO_3 solution and EtOAc (pH 7–8) and extracted. The organic phase was washed with KF solution, dried over $MgSO_4$, and evaporated. The crude solid was purified by column chromatography (petroleum ether/EtOAc, 7:3) to give **4f** (48 mg, 89%). Mp 118–120 °C (CH_2Cl_2/petroleum ether). IR (KBr): ν 3127, 2981, 1686, 1586, 1528, 1496, 1376, 1300, 1172, 1121, 817, 748 cm^{-1}. ^1H NMR (300 MHz, $CDCl_3$): δ 1.43 (d, 6H, $J = 6.0$ Hz, CH_3), 2.65 (s, 3H, CH_3), 4.78 (hept, 1H, $J = 6.0$ Hz, CH), 6.69 (d, 1H, $J = 6.0$ Hz, H-5), 7.51 (broad t, 2H, $J = 7.9$ Hz, H_{arom}), 7.61 (broad t, 1H, $J = 7.9$ Hz, H_{arom}), 8.17 (s, 1H, H-2), 8.23 (broad d, 2H, $J = 7.9$ Hz, H_{arom}), 8.29 (d, 1H, $J = 6.0$ Hz, H-6). MS (IS): *m/z* 359 ($M + H^+$). Anal. ($C_{18}H_{18}N_2O_4S$) C, H, N.

3-Acetyl-4-methoxy-1-methyl-1*H*-pyrrolo[2,3-*b*]pyridine (4g). Under an inert atmosphere, a solution of **3b** (80 mg, 0.42 mmol), dimethyl sulfate (0.07 mL, 0.74 mmol), and K_2CO_3 (82 mg, 0.59 mmol) in dry acetone (15 mL) was refluxed for 5.5 h. After the mixture was cooled, solvent was evaporated. The residue was partitioned between H_2O and EtOAc (30 mL, 1:1) and extracted. The organic phase was dried over $MgSO_4$ and evaporated. The crude residue was purified by column chromatography (EtOAc) to give **4g** (70 mg, 81%). Mp 79–81 °C (CH_2Cl_2/hexane). IR (KBr): ν 3123, 2984, 1649, 1590, 1573, 1521, 1448, 1335, 1313, 1285, 1239, 1199, 1083, 1054, 961, 800 cm^{-1}. ^1H NMR (300 MHz, $CDCl_3$): δ 2.61 (s, 3H, CH_3), 3.85 (s, 3H, CH_3), 3.99 (s, 3H, CH_3), 6.64 (d, 1H, $J = 5.5$ Hz, H-5), 7.76 (s, 1H, H-2), 8.23 (d, 1H, $J = 5.5$ Hz, H-6). MS (IS): *m/z* 205 ($M + H^+$). Anal. ($C_{11}H_{12}N_2O_2$) C, H, N.

1-(1-Benzenesulfonyl-4-chloro-1*H*-pyrrolo[2,3-*b*]pyridin-3-yl)-3-dimethylaminopropenone (7a). Under an inert atmosphere, a solution of **4a** (450 mg, 1.34 mmol) and DMF-DMA (1.07 mL, 8.0 mmol) in dry DMF (15 mL) was stirred at 90 °C for 8 h. After the mixture was cooled, the solvent was evaporated under reduced pressure. The residue was partitioned between H_2O and EtOAc (50 mL, 1:1) and extracted. The organic phase was dried over $MgSO_4$ and evaporated. The crude solid was purified by column chromatography (EtOAc) to give **7a** (310 mg, 60%). Mp 139–141 °C (MeOH). IR (KBr): ν 3132, 3021, 2902, 1646, 1562, 1526, 1381, 1169, 989, 885, 728 cm^{-1}. ^1H NMR (300 MHz, $CDCl_3$): δ 2.93 (broad s, 3H, CH_3), 3,15 (broad s, 3H, CH_3), 5.49 (d, 1H, $J = 12.6$ Hz, =CH), 7.23 (d, 1H, $J = 5.3$ Hz, H-5), 7.49 (t, 2H, $J = 7.4$ Hz, H_{arom}), 7.47–7.65 (m, 2H, H_{arom} + =CH), 8.00 (s, 1H, H-2), 8.19 (d, 2H, $J = 7.7$ Hz, H_{arom}), 8.29 (d, 1H, $J = 5.3$ Hz, H-6). MS (IS): *m/z* 390 ($M + H^+$). Anal. ($C_{18}H_{16}ClN_3O_3S$) C, H, N.

1-(1-Benzenesulfonyl-4-methoxy-1*H*-pyrrolo[2,3-*b*]pyridin-3-yl)-3-dimethylaminopropenone (7b). According to the same procedure, compound **7b** was obtained in 78% yield from **4b**. Mp 210–212 °C (MeOH). IR (KBr): ν 3144, 2950, 1632, 1578, 1544, 1414, 1371, 1294, 1193, 1166, 888, 798 cm^{-1}. ^1H NMR (300 MHz, $CDCl_3$): δ 2.91 (broad s, 3H, CH_3), 3.12 (broad s, 3H, CH_3), 3.94 (s, 3H, CH_3), 5.62 (d, 1H, $J = 12.6$ Hz, =CH), 6.68 (d, 1H, $J =$

5.7 Hz, H-5), 7.47 (t, 2H, $J = 7.4$ Hz, H_{arom}), 7.57 (t, 1H, $J = 7.4$ Hz, H_{arom}), 7.65 (broad d, 1H, $J = 12.6$ Hz, =CH), 7.96 (s, 1H, H-2), 8.18 (d, 2H, $J = 7.4$ Hz, H_{arom}), 8.31 (d, 1H, $J = 5.7$ Hz, H-6). MS (IS): *m/z* 386 ($M + H^+$). Anal. ($C_{19}H_{19}N_3O_4S$) C, H, N.

1-(1-Benzenesulfonyl-6-bromo-1*H*-pyrrolo[2,3-*b*]pyridin-3-yl)-3-dimethylaminopropenone (7c). According to the same procedure, compound **7c** was obtained in 62% yield from **4c**. Mp 181–183 °C (MeOH). IR (KBr): ν 3142, 3070, 2912, 1643, 1569, 1555, 1526, 1391, 1279, 1172, 1085, 1034, 964, 889, 817 cm^{-1}. ^1H NMR (300 MHz, $CDCl_3$): δ 2.89 (broad s, 3H, CH_3), 3.10 (broad s, 3H, CH_3), 5.52 (d, 1H, $J = 12.2$ Hz, =CH), 7.34 (d, 1H, $J = 8.2$ Hz, H-5), 7.49 (t, 2H, $J = 7.5$ Hz, H_{arom}), 7.58 (t, 1H, $J = 7.5$ Hz, H_{arom}), 7.72 (d, 1H, $J = 12.2$ Hz, =CH), 8.15 (s, 1H, H-2), 8.26 (d, 2H, $J = 7.5$ Hz, H_{arom}), 8.44 (d, 1H, $J = 8.2$ Hz, H-4). MS (IS): *m/z* 436 (^{81}Br, $M + H^+$), 434 (^{79}Br, $M + H^+$). Anal. ($C_{18}H_{16}BrN_3O_3S$) C, H, N.

1-(1-Benzenesulfonyl-4-ethoxy-1*H*-pyrrolo[2,3-*b*]pyridin-3-yl)-3-dimethylaminopropenone (7d). According to the same procedure, compound **7d** was obtained in 68% yield from **4d**. Mp 187–189 °C (MeOH). IR (KBr): ν 3146, 2985, 1636, 1576, 1536, 1420, 1368, 1293, 1279, 1166, 1105, 893, 787 cm^{-1}. ^1H NMR (300 MHz, $CDCl_3$): δ 1.44 (t, 3H, $J = 7.2$ Hz, CH_3), 2.90 (broad s, 3H, CH_3), 3.11 (broad s, 3H, CH_3), 4.18 (q, 2H, $J = 7.2$ Hz, CH_2), 5.60 (d, 1H, $J = 12.6$ Hz, =CH), 6.65 (d, 1H, $J = 5.6$ Hz, H-5), 7.46 (t, 2H, $J = 7.1$ Hz, H_{arom}), 7.55–7.63 (m, 2H, H_{arom} + =CH), 7.94 (s, 1H, H-2), 8.18 (d, 2H, $J = 7.7$ Hz, H_{arom}), 8.29 (d, 1H, $J = 5.6$ Hz, H-6). MS (IS): *m/z* 400 ($M + H^+$). Anal. ($C_{20}H_{21}N_3O_4S$) C, H, N.

1-(1-Benzenesulfonyl-4-propoxy-1*H*-pyrrolo[2,3-*b*]pyridin-3-yl)-3-dimethylaminopropenone (7e). According to the same procedure, compound **7e** was obtained in 69% yield from **4e**. Mp 139–141 °C (CH_2Cl_2/pentane). IR (KBr): ν 3140, 2932, 1638, 1575, 1551, 1370, 1295, 1280, 1190, 1170, 1110, 1083, 897, 737 cm^{-1}. ^1H NMR (300 MHz, $CDCl_3$): δ 1.02 (t, 3H, $J = 7.3$ Hz, CH_3), 1.77–1.89 (m, 2H, CH_2), 2.90 (broad s, 3H, CH_3), 3.10 (broad s, 3H, CH_3), 4.05 (q, 2H, $J = 6.4$ Hz, CH_2), 5.59 (d, 1H, $J = 12.6$ Hz, =CH), 6.64 (d, 1H, $J = 5.6$ Hz, H-5), 7.46 (t, 2H, $J = 7.4$ Hz, H_{arom}), 7.56 (broad t, 1H, $J = 7.4$ Hz, H_{arom}), 7.62 (broad d, 1H, $J = 12.6$ Hz, =CH), 7.91 (s, 1H, H-2), 8.18 (d, 2H, $J = 7.4$ Hz, H_{arom}), 8.28 (d, 1H, $J = 5.6$ Hz, H-6). MS (IS): *m/z* 414 ($M + H^+$). Anal. ($C_{21}H_{23}N_3O_4S$) C, H, N.

1-(1-Benzenesulfonyl)-4-(1-methylethoxy)-1*H*-pyrrolo[2,3-*b*]pyridin-3-yl)-3-dimethylaminopropenone (7f). According to the same procedure, compound **7f** was obtained in 69% yield from **4f**. Mp 150–152 °C (MeOH). IR (KBr): ν 3150, 2925, 1638, 1552, 1495, 1373, 1290, 1190, 1168, 1110, 895 cm^{-1}. ^1H NMR (300 MHz, $CDCl_3$): δ 1.37 (d, 6H, $J = 6.0$ Hz, CH_3), 2.95 (broad s, 3H, CH_3), 3.14 (broad s, 3H, CH_3), 4.72 (hept, 1H, $J = 6.0$ Hz, CH), 5.68 (broad d, 1H, $J = 12.5$ Hz, =CH), 6.65 (d, 1H, $J = 5.7$ Hz, H-5), 7.47 (t, 2H, $J = 7.5$ Hz, H_{arom}), 7.57 (t, 1H, $J = 7.5$ Hz, H_{arom}), 7.73–7.79 (m, 1H, =CH), 7.98 (s, 1H, H-2), 8.20 (d, 2H, $J = 7.5$ Hz, H_{arom}), 8.28 (d, 1H, $J = 5.7$ Hz, H-6). MS (IS): *m/z* 414 ($M + H^+$). Anal. ($C_{21}H_{23}N_3O_4S$) C, H, N.

1-(4-Methoxy-1-methyl-1*H*-pyrrolo[2,3-*b*]pyridin-3-yl)-3-dimethylaminopropenone (7g). According to the same procedure, compound **7g** was obtained in 82% yield from **4g**. Mp 138–140 °C (MeOH). IR (KBr): ν 3116, 3014, 2906, 1631, 1531, 1503, 1418, 1355, 1282, 1232, 1184, 1072, 887, 789 cm^{-1}. ^1H NMR (300 MHz, $CDCl_3$): δ 3.00 (broad s, 6H, CH_3), 3.87 (s, 3H, CH_3), 4.00 (s, 3H, CH_3), 6.08 (d, 1H, $J = 12.6$ Hz, =CH), 6.63 (d, 1H, $J = 5.6$ Hz, H-5), 7.74 (d, 1H, $J = 12.6$ Hz, =CH), 7.76 (s, 1H, H-2), 8.23 (d, 1H, $J = 5.6$ Hz, H-6). MS (IS): *m/z* 260 ($M + H^+$). Anal. ($C_{14}H_{17}N_3O_2$) C, H, N.

3-[(2-Amino)pyrimidin-4-yl]-4-chloro-1*H*-pyrrolo[2,3-*b*]pyridine (1a). Meriolin 10. A solution of **7a** (140 mg, 0.36 mmol), guanidine·HCl (52 mg, 0.54 mmol), and K_2CO_3 (106 mg, 0.76 mmol) in 2-methoxyethanol (5 mL) was heated at 100–110 °C for 36 h. After the mixture was cooled, the solution was poured into H_2O. The final solution was extracted by EtOAc twice. The organic phase was dried over $MgSO_4$ and evaporated under reduced pressure. The residue was purified by column chromatography (CH_2Cl_2/MeOH, 95:5) to afford **1a** (45 mg, 51%) and **1 h** (32 mg, 31%). Mp >210 °C (MeOH). IR (KBr): ν3310, 3135, 3021, 2852, 1659, 1563, 1515, 1459, 1398, 1311 cm^{-1}. ^1H NMR (300 MHz, DMSO-d_6): δ 6.48 (broad s, 2H, NH_2), 6.85 (d, 1H, $J = 5.3$ Hz, H-5), 7.26 (d, 1H, $J = 5.3$ Hz, H-5′), 7.94 (s, 1H, H-2), 8.20 (d, 1H, $J = 5.3$ Hz, H-6), 8.22 (d, 1H, $J = 5.3$ Hz, H-6′), 12.49 (broad s, 1H, NH), MS (IS): *m/z* 246 ($M + H^+$). Anal. ($C_{11}H_8ClN_5$) C, H, N.

3-[(2-Amino)pyrimidin-4-yl]-4-(2-methoxyethoxy)-1*H*-pyrrolo[2,3-*b*]pyridine (1h). Meriolin 7. Compound **1h** was obtained in 31% yield from **7a**. Mp 172–174 °C (MeOH). IR (KBr): ν 3314, 3182, 3097, 2924, 1640, 1575, 1465, 1401, 1326 cm^{-1}. ^1H NMR (300 MHz, DMSO-d_6): δ 3.70 (t, 2H, $J = 5.1$ Hz, CH_2), 3.99 (s, 3H, CH_3), 4.46 (t, 2H, $J = 5.1$ Hz, CH_2), 6.37 (broad s, 2H, NH_2), 6.84 (d, 1H, $J = 5.6$ Hz, H-5), 7.28 (d, 1H, $J = 5.3$ Hz, H-5′), 8.03 (s, 1H, H-2), 8.18 (d, 1H, $J = 5.3$ Hz, H-6′), 8.21 (d, 1H, $J = 5.6$ Hz, H-6), 12.49 (broad s, 1H, NH). MS (IS): *m/z* 286 ($M + H^+$). Anal. ($C_{14}H_{15}N_5O_2$) C, H, N.

3-[(2-Amino)pyrimidin-4-yl]-4-methoxy-1*H*-pyrrolo[2,3-*b*]pyridine (1b). Meriolin 3. According to the same procedure, compound **1b** was obtained in 75% yield from **7b**. Mp >210 °C (MeOH). IR (KBr): ν 3326, 3148, 3014, 1638, 1574, 1503, 1453, 1310, 1097 cm^{-1}. ^1H NMR (300 MHz, DMSO-d_6): δ 3.97 (s, 3H, CH_3), 6.32 (broad s, 2H, NH_2), 6.79 (d, 1H, $J = 5.5$ Hz, H-5), 7.27 (d, 1H, $J = 5.3$ Hz, H-5′), 7.92 (s, 1H, H-2), 8.16 (d, 1H, $J = 5.5$ Hz, H-6), 8.17 (d, 1H, $J = 5.3$ Hz, H-6′), 12.13 (broad s, 1H, NH). MS (IS): *m/z* 242 ($M + H^+$). Anal. ($C_{12}H_{11}N_5O$) C, H, N.

3-[(2-Amino)pyrimidin-4-yl]-6-bromo-1*H*-pyrrolo[2,3-*b*]pyridine (1c). Meriolin 11. According to the same procedure, compound **1c** was obtained in 68% yield from **7c**. Mp >210 °C (MeOH). IR (KBr): ν 3303, 3130, 2886, 1658, 1575, 1555, 1509, 1454, 1421, 1308, 1271, 1114 cm^{-1}. ^1H NMR (300 MHz, DMSO-d_6): δ 6.54 (broad s, 2H, NH_2), 7.05 (d, 1H, $J = 5.3$ Hz, H-5′), 7.36 (d, 1H, $J = 8.3$ Hz, H-5), 8.15 (d, 1H, $J = 5.3$ Hz, H-6′), 8.38 (s, 1H, H-2), 8.87 (d, 1H, $J = 8.3$ Hz, H-4), 12.42 (broad s, 1H, NH). MS (IS): *m/z* 292 (Br^{81}, $M + H^+$), 290 (^{79}Br, $M + H^+$). Anal. ($C_{11}H_8BrN_5$) C, H, N.

3-[(2-Amino)pyrimidin-4-yl]-4-ethoxy-1*H*-pyrrolo[2,3-*b*]pyridine (1d). Meriolin 4. According to the same procedure, compound **1d** was obtained in 63% yield from **7d**. Mp >210 °C (MeOH). IR (KBr): ν 3338, 3167, 1653, 1578, 1570, 1500, 1439, 1410, 1390, 1310, 1092, 1014 cm^{-1}. ^1H NMR (300 MHz, DMSO-d_6): δ 1.45 (t, 3H, $J = 7.2$ Hz, CH_3), 4.26 (q, 2H, $J = 7.2$ Hz, CH_2), 6.33 (broad s, 2H, NH_2), 6.75 (d, 1H, $J = 5.5$ Hz, H-5), 7.36 (d, 1H, $J = 5.3$ Hz, H-5′), 7.90 (s, 1H, H-2), 8.13 (d, 1H, $J = 5.5$ Hz, H-6), 8.17 (d, 1H, $J = 5.3$ Hz, H-6′), 12.09 (broad s, 1H, NH). MS (IS): *m/z* 256 ($M + H^+$). Anal. ($C_{13}H_{13}N_5O$) C, H, N.

3-[(2-Amino)pyrimidin-4-yl]-4-propoxy-1*H*-pyrrolo[2,3-*b*]pyridine (1e). Meriolin 5. According to the same procedure, compound **1e** was obtained in 60% yield from **7e**. Mp >210 °C (MeOH). IR (KBr): ν 3327, 3158, 2937, 1649, 1566, 1500, 1451, 1409, 1309, 1091 cm^{-1}. ^1H NMR (300 MHz, DMSO-d_6): δ 1.01 (t, 3H, $J = 7.3$ Hz, CH_3), 1.81–1.90 (m, 2H, CH_2), 4.16 (t, 2H, $J = 6.2$ Hz, CH_2), 6.32 (broad s, 2H, NH_2), 6.76 (d, 1H, $J = 5.5$ Hz, H-5), 7.34 (d, 1H, $J = 5.3$ Hz, H-5′), 7.90 (s, 1H, H-2), 8.14 (d, 1H, $J = 5.5$ Hz, H-6), 8.16 (d, 1H, $J = 5.3$ Hz, H-6′), 12.07 (broad s, 1H, NH). MS (IS): *m/z* 270 ($M + H^+$) Anal. ($C_{14}H_{15}N_5O$) C, H, N.

3-[(2-Amino)pyrimidin-4-yl]-4-(1-methylethoxy)-1*H*-pyrrolo[2,3-*b*]pyridine (1f). Meriolin 6. According to the same procedure, compound **1f** was obtained in 60% yield from **7f**. Mp >210 °C (MeOH). IR (KBr): ν 3323, 3168, 2921, 1655, 1570, 1510, 1462, 1305, 1105 cm^{-1}. ^1H NMR (300 MHz, DMSO-d_6): δ 1.39 (d, 6H, $J = 6.0$ Hz, CH_3), 4.91 (hept, 1H, $J = 6.0$ Hz, CH), 6.30 (broad s, 2H, NH_2), 6.77 (d, 1H, $J = 5.6$ Hz, H-5), 7.34 (d, 1H, $J = 5.3$ Hz, H-5′), 7.87 (s, 1H, H-2), 8.11 (d, 1H, $J = 5.6$ Hz, H-6), 8.17 (d, 1H, $J = 5.3$ Hz, H-6′), 12.03 (broad s, 1H, NH). MS (IS): *m/z* 270 ($M + H^+$). Anal. ($C_{14}H_{15}N_5O$) C, H, N.

3-[(2-Amino)pyrimidin-4-yl]-4-methoxy-1-methyl-1*H*-pyrrolo[2,3-*b*]pyridine (1g). Meriolin 9. According to the same procedure, compound **1g** was obtained in 92% yield from **7g**. Mp >210

°C (MeOH). IR (KBr): ν 3347, 3312, 3177, 2985, 1640, 1599, 1572, 1522, 1458, 1327, 1304, 1284, 1201, 1074 cm^{-1}. ^1H NMR (300 MHz, $CDCl_3$): δ 3.91 (s, 3H, CH_3), 4.02 (s, 3H, CH_3), 4.93 (broad s, 2H, NH_2), 6.65 (d, 1H, $J = 5.5$ Hz, H-5), 7.45 (d, 1H, $J = 5.3$ Hz, H-5′), 7.92 (s, 1H, H-2), 8.26 (d, 1H, $J = 5.3$ Hz, H-6′), 8.27 (d, 1H, $J = 5.5$ Hz, H-6). MS (IS): m/z 256 ($M + H^+$). Anal. ($C_{13}H_{13}N_5O$) C, H, N.

3-[(2-Amino)pyrimidin-4-yl]-4-hydroxy-1*H*-pyrrolo[2,3-*b*]pyridine (8). Meriolin 2. A solution of **1b** (50 mg, 0.20 mmol) in 48% HBr/AcOH (6 mL) was refluxed for 2 h. After the mixture was cooled, solvent was evaporated. The residue was dissolved in EtOAc (10 mL), and then the solution was neutralized by addition of saturated aqueous Na_2CO_3 (pH 7–8). The phases were separated, and the aqueous phase was washed by EtOAc twice (2 × 10 mL). The combined organic phases were dried over $MgSO_4$ and evaporated under reduced pressure. The solid obtained was recrystallized from methanol to afford **8** (43 mg, 90%). Mp >210 °C (MeOH). IR (KBr): ν 3478, 3303, 3082, 2827, 1643, 1581, 1461, 1392, 1287, 1225, 1156 cm^{-1}. ^1H NMR (300 MHz, DMSO-d_6 + D_2O): δ 6.51 (d, 1H, $J = 5.5$ Hz, H-5), 7.15 (d, 1H, $J = 5.5$ Hz, H-5′), 7.99 (d, 1H, $J = 5.5$ Hz, H-6), 8.17 (d, 1H, $J = 5.5$ Hz, H-6′), 8.24 (s, 1H, H-2). MS (IS): m/z 228 ($M + H^+$). Anal. ($C_{11}H_9N_5O$) C, H, N.

3-[(2-Amino)pyrimidin-4-yl]-4-hydroxy-1-methyl-1*H*-pyrrolo[2,3-*b*]pyridine (9). Meriolin 8. According to the same procedure, compound **9** was obtained in 92% yield from **1g**. Mp >210 °C (MeOH). IR (KBr): ν 3440, 3310, 3170, 2929, 1647, 1573, 1542, 1497, 1326, 1290, 1223, 1186, 1173 cm^{-1}. ^1H NMR (300 MHz, DMSO-d_6 + D_2O): δ 3.78 (s, 3H, CH_3), 6.56 (d, 1H, $J = 5.5$ Hz, H-5), 7.08 (d, 1H, $J = 5.5$ Hz, H-5′), 8.04 (d, 1H, $J = 5.5$ Hz, H-6), 8.16 (d, 1H, $J = 5.5$ Hz, H-6′), 8.28 (s, 1H, H-2). MS (IS): m/z 242 ($M + H^+$). Anal. ($C_{12}H_{11}N_5O$) C, H, N.

3-Pyrimidin-4-yl-4-methoxy-1*H*-pyrrolo[2,3-*b*]pyridine (10). Meriolin 14. A solution of 4-methoxy-7-azaindole **2b** (100 mg, 0.67 mmol), CuCl (27 mg, 0.27 mmol), and formamide (300 μL) was heated at 170 °C for 18 h. After the mixture was cooled, water was added to the solution (pH 9) and extraction was performed with EtOAc. The organic phase was dried over $MgSO_4$ and evaporated. The crude residue was purified by column chromatography (EtOAc/MeOH, 9:1) to afford **10** (40 mg, 26%). Mp >210 °C (MeOH). IR (KBr): ν 3083, 3021, 2923, 2851, 1575, 1544, 1354, 1299, 1093 cm^{-1}. ^1H NMR (300 MHz, CD_3OD + D_2O): δ 4.09 (s, 3H, CH_3), 6.88 (d, 1H, $J = 5.6$ Hz, H-5), 8.12 (s, 1H, H-2), 8.20–8.22 (m, 2H, H-5′, H-6), 8.65 (d, 1H, $J = 5.3$ Hz, H-6′), 8.99 (s, 1H, H-2′). MS (IS): m/z 227 ($M + H^+$). Anal. ($C_{12}H_{10}N_4O$) C, H, N.

3-(Pyrimidin-4-yl)-4-hydroxy-1*H*-pyrrolo[2,3-*b*]pyridine (11). Meriolin 13. According to the same procedure described for the preparation of **8**, compound **11** was obtained in 92% yield from **10**. Mp >210 °C (MeOH). IR (KBr): ν 3429, 3078, 2923, 2851, 1636, 1592, 1554, 1463, 1406, 1308, 1290, 1157, 1011 cm^{-1}. ^1H NMR (300 MHz, DMSO-d_6): δ 6.53 (d, 1H, $J = 5.1$ Hz, H-5), 8.05 (d, 1H, $J = 5.1$ Hz, H-6), 8.12 (d, 1H, $J = 5.6$ Hz, H-5′), 8.58 (s, 1H, H-2), 8.71 (d, 1H, $J = 5.6$ Hz, H-6′), 9.10 (s, 1H, H-2′), 12.42 (broad s, 1H, NH), 14.24 (s, 1H, OH). MS (IS): m/z 213 ($M + H^+$). Anal. ($C_{11}H_8N_4O$) C, H, N.

3-[(2-Methylsulfanyl)pyrimidin-4-yl]-4-methoxy-1*H*-pyrrolo[2,3-*b*]pyridine (12). Meriolin 12. According to the same procedure described for the preparation of **1a**, compound **12** was obtained in 30% yield from **7b** and 2-methyl-2-thiopseudourea sulfate (time reaction = 5 days). Mp >210 °C. IR (KBr): ν 3134, 3083, 2900, 2840, 1585, 1556, 1468, 1415, 1363, 1306, 1202, 1095 cm^{-1}. ^1H NMR (300 MHz, DMSO-d_6): δ 2.55 (s, 3H, CH_3), 4.01 (s, 3H, CH_3), 6.84 (d, 1H, $J = 5.5$ Hz, H-5), 7.84 (d, 1H, $J = 5.5$ Hz, H-5′), 8.18 (s, 1H, H-2), 8.21 (d, 1H, $J = 5.5$ Hz, H-6), 8.50 (d, 1H, $J = 5.5$ Hz, H-6′), 12.38 (broad s, 1H, NH). MS (IS): m/z 273 ($M + H^+$). Anal. ($C_{13}H_{12}N_4OS$) C, H, N.

Crystallography. Expression, Purification, and Cocrystallization of Human CDK2/Cyclin A with Meriolins 3 (1b) and 5 (1e) and Variolin B. Thr160-phosphorylated CDK2/cyclin A3 complex was purified as described previously[67] and concentrated to 13 mg/mL in 40 mM HEPES, pH 7.0, 200 mM NaCl, 0.01% monothioglycerol. The protein solution was incubated 20 min on ice with meriolin 5 (0.8 mM), meriolin 3 (1.8 mM), or variolin B (1.8 mM) before setting up hanging drop crystallization trials. The reservoir solution contained 0.6–0.8 M KCl, 0.9–1.2 M $(NH_4)_2SO_4$, and 100 mM HEPES, pH 7.0. Orthorhombic crystals grew within 3 weeks at 4 °C. Crystals were briefly soaked in 8 M sodium formate before being frozen in liquid nitrogen.

X-ray Crystallography Data Collection and Processing, Structure Solution, and Structure Refinement. Data were collected on a single crystal of each CDK2/cyclin A/inhibitor complex at 100 K at either the Elettra beamline X-ray diffraction (for meriolin 5) or the ESRF ID14-EH-2 (for meriolin 3 and variolin B). Data processing and integration were carried out using MOSFLM and SCALA.[68] The structures were solved by molecular replacement with MOLREP using a well refined structure of CDK2/cyclin A3 (unpublished results) as the search model. Two CDK2/cyclin A dimers were found in the asymmetric unit. Within each electron density map, strong electron density corresponding to the bound inhibitor was seen at the ATP site after rigid body refinement. The structure refinement to 2.30 Å for meriolin 5, 2.0 Å for meriolin 3, and 2.10 Å for variolin B and the inhibitor model building were performed using the CCP4 software suite.[68] Alternate cycles of rebuilding in Coot[69] and refinement in Refmac[70] were carried out to obtain the final models. Data collection and refinement statistics are presented in Table 1. The structures of CDK2/cyclin A/meriolin 3, CDK2/cyclin A/meriolin 5, and CDK2/cyclin A/variolin B have been deposited in the PDB with accession codes 3BHT, 3BHU, and 3BHV, respectively.

Protein Kinase Assays. Biochemical Reagents. Sodium orthovanadate, EGTA, EDTA, Mops, β-glycerophosphate, phenyl phosphate, sodium fluoride, dithiothreitol (DTT), glutathione-agarose, glutathione, bovine serum albumin (BSA), nitrophenyl phosphate, leupeptin, aprotinin, pepstatin, soybean trypsin inhibitor, benzamidine, and histone H1 (type III-S) were obtained from Sigma Chemicals. [γ-^{33}P]ATP was obtained from Amersham. The GSK-3-specific substrate GS-1 (YRRAAVPPSPSLSRHSSPHQSpEDEEE) and the CK1-specific peptide substrate (RRKHAAIGSpAYSITA)[71] were synthesized by the Peptide Synthesis Unit, Millegen, Prologue Biotech, Labege, France.

Buffers. Homogenization buffer consisted of 60 mM β-glycerophosphate, 15 mM *p*-nitrophenyl phosphate, 25 mM Mops (pH 7.2), 15 mM EGTA, 15 mM $MgCl_2$, 1 mM DTT, 1 mM sodium vanadate, 1 mM NaF, 1 mM phenylphosphate, 10 μg of leupeptin/mL, 10 μg of aprotinin/mL, 10 μg of soybean trypsin inhibitor/mL, and 100 μM benzamidine.

Buffer A consisted of 10 mM $MgCl_2$, 1 mM EGTA, 1 mM DTT, 25 mM Tris-HCl, pH 7.5, and 50 μg of heparin/mL.

Buffer C consisted of homogenization buffer but 5 mM EGTA, no NaF, and no protease inhibitors.

Kinase Preparations and Assays. Kinase activities were assayed in buffer A or C at 30 °C at a final ATP concentration of 15 μM. Blank values were subtracted and activities calculated as picomoles of phosphate incorporated for a 30 min incubation. The activities are usually expressed as percent of the maximal activity, i.e., in the absence of inhibitors. Controls were performed with appropriate dilutions of dimethyl sulfoxide.

CDK1/cyclin B was extracted in homogenization buffer from M phase starfish (*Marthasterias glacialis*) oocytes and purified by affinity chromatography on $p9^{CKShs1}$-sepharose beads, from which it was eluted by free $p9^{CKShs1}$ as previously described.[72] The kinase activity was assayed in buffer C, with 1 mg of histone H1/mL, in the presence of 15 μM [γ-^{33}P]ATP (3000 Ci/mmol, 10 mCi/mL) in a final volume of 30 μL. After 30 min of incubation at 30 °C, 25 μL aliquots of supernatant were spotted onto Whatman P81 phosphocellulose paper filters, and 20 s later, the filters were washed five times (for at least 5 min each time) in a solution of 10 mL of phosphoric acid/L of water. The wet filters were counted in the presence of ACS (Amersham) scintillation fluid.

CDK2/cyclin A (human, recombinant, expressed in insect cells) was assayed as described for CDK1/cyclin B.

CDK5/p25 was reconstituted by mixing equal amounts of recombinant mammalian CDK5 and p25 expressed in *E. coli* as GST (glutathione-*S*-transferase) fusion proteins and purified by affinity chromatography on glutathione-agarose (vectors kindly provided by Dr. L. H. Tsai) (p25 is a truncated version of p35, the 35 kDa CDK5 activator). Its activity was assayed with histone H1 in buffer C as described for CDK1/cyclin B.

CDK9/cyclin T (human, recombinant, expressed in insect cells) was assayed as described for CDK1/cyclin B but using a pRB fragment (aa773–928) (3.5 μg/assay) as a substrate.

GSK-3α/β was purified from porcine brain by affinity chromatography on immobilized axin.[73] It was assayed, following a $^1/_{100}$ dilution in 1 mg of BSA/mL of 10 mM DTT, with 5 μL of 4 μM GS-1 peptide substrate, in buffer A, in the presence of 15 μM [γ-^{33}P]ATP (3000 Ci/mmol, 10 mCi/mL) in a final volume of 30 μL. After 30 min of incubation at 30 °C, 25 μL aliquots of supernatant were processed as described above.

CK1δ/ϵ was purified from porcine brain by affinity chromatography on an immobilized axin fragment.[74] It was assayed as described for CDK1 but using a CK1-specific peptide substrate.

DYRK1A (rat, recombinant, expressed in *E. coli* as a GST fusion protein) was purified by affinity chromatography on glutathione-agarose and assayed as described for CDK1/cyclin B.

Cell Biology. Antibodies and Chemicals. CelTiter 96 kit containing the MTS reagent was purchased from Promega (Madison, WI). The protease inhibitor cocktail was from Roche, and fetal calf serum (FCS) was from Invitrogen. Unless otherwise stated, the nonlisted reagents were from Sigma.

Cell Lines and Culture Conditions. SH-SY5Y human neuroblastoma cell line was grown in DMEM with L-glutamine medium from Invitrogen (Cergy Pontoise, France), antibiotics, and 10% volume of FCS from Invitrogen.

HEK293 cells were grown in MEM with Glutamax medium from Invitrogen, antibiotics, and 10% volume of FCS.

KMS-11, a multiple myeloma adherent cell line,[75] and GBM, a multiform glioblastoma primary culture,[76] were grown in cultured in RPMI 1640 medium supplemented with 5% and 10% fetal calf serum, respectively, 2 mM glutamine, antibiotics (100 IU/mL penicillin and 100 μg/mL streptomycin), and 10 μM β-mercaptoethanol (Life Technologies). Cells were subcultured at confluency after dispersal with 0.025% trypsin in 0.02% EDTA. For experiments cells were used at 70−80% confluence.

General culture conditions were an atmosphere of 5% CO_2 and a temperature of 37 °C.

Culture dishes and other plastic disposable tools were supplied by Corning (Corning, NY). Drug treatments were performed on exponentially growing cultures at the indicated time and concentrations. Control experiments were also carried out using appropriate dilutions of DMSO.

Cell Viability Assessment. Cell viability was determined by measuring the reduction of 3-(4,5-dimethylthiazol-2-yl)-5-(3-carboxymethoxyphenyl)-2-(4-sulfophenyl)-2 *H*-tetrazolium (MTS). The procedure has been previously described in detail.[77]

Alternatively, cell viability was assessed by the neutral red uptake assay (KMS-11 and GBM cells). The 20 000 cells were plated in 96-well culture microtiter plates (Falcon) and incubated at 37 °C in 5% CO_2. After 24 h drugs were added in fresh medium, and after 48 h cells were loaded for 3 h with 50 μg of neutral red/mL. This weakly cationic dye penetrates cell membranes by nonionic diffusion and binds intracellularly to anionic carboxylic and/or phosphate groups of the lysosomal matrix. Thereafter, the medium was removed, cells were fixed for 5 min with a mixture of 1% formaldehyde and 1% $CaCl_2$, and the dye was extracted with 0.2 mL of 1% acetic acid in 50% ethanol. Plates were left overnight at 4 °C, and absorbance was recorded at 570 nm (Multiskan EX, Thermo-Electron Corporation) and corrected with a blank. Experiments were performed at least in triplicate, four wells being used per cell line.

Preparation and Analysis of Cell Spheroids. We have adapted the hanging-drop method[64] to produce parental HCT116 spheroids of homogeneous diameter. The 25 μL drops containing 500 cells were suspended on the lid of agar-coated 24-well dishes containing 1 mL of culture media. After the 72 h period required for cell aggregation, the spheroids were transferred to the culture medium. Spheroids were treated with different concentrations of meriolin 3, 4 days after the start of the culture and for a 5 day period. The size of three spheroids per experimental condition was determined at day 0 (V_0) and day 5 (V_5) by measuring two orthogonal diameters (d_1 and d_2) using an inverted microscope fitted with a calibrated eyepiece reticule. Volumes were determined according to the formula $V = (^4/_3)\pi r^3$ where $r = (^1/_2)(d_1 d_2)^{1/2}$. Each experiment was repeated three times.

Acknowledgment. We are grateful to Dr. J. Boix for the SH-SY5Y cell line, to Tristan Gallenne for GBM cells, and to the beamline scientists at the ESRF (ID14-2) and at beamline X-ray diffraction Elettra for providing excellent facilities for crystal data collection. This research was supported by grants from the EEC (Grant FP6-2002, Life Sciences & Health, PROKINASE Research Project) (L.M., J.A.E.), "Cancéropole Grand-Ouest" (L.M.), and the Australian Research Council (J.C.M). K.B. was supported by a fellowship from the "Ministère de la Recherche".

Supporting Information Available: Results from elemental analysis and detailed comparative analysis of the cocrystal structures. This material is available free of charge via the Internet at http://pubs.acs.org.

References

(1) Malumbres, M.; Barbacid, M. Mammalian cyclin-dependent kinases. *Trends Biochem. Sci.* **2005**, *30*, 630–641.
(2) Camins, A.; Verdaguer, E.; Folch, J.; Canudas, A. M.; Pallas, M. The role of CDK5/P25 formation/inhibition in neurodegeneration. *Drug News Perspect.* **2006**, *19*, 453–460.
(3) Pareek, T. K.; Keller, J.; Kesavapany, S.; Pant, H. C.; Iadarola, M. J.; Brady, R. O.; Kulkarni, A. B. Cyclin-dependent kinase 5 activity regulates pain signaling. *Proc. Natl. Acad. Sci. U.S.A.* **2006**, *103*, 791–796.
(4) Borgne, A.; Versteege, I.; Mahé, M.; Studeny, A.; Léonce, S.; Naime, I.; Rodriguez, M.; Hickman, J. A.; Meijer, L.; Golsteyn, R. M. Analysis of cyclin B1 and CDK activity during apoptosis induced by camptothecin treatment. *Oncogene* **2006**, *25*, 7361–7372.
(5) Garriga, J.; Grana, X. Cellular control of gene expression by T-type cyclin/CDK9 complexes. *Gene* **2004**, *337*, 15–23.
(6) Loyer, P.; Trembley, J. H.; Katona, R.; Kidd, V. J.; Lahti, J. M. Role of CDK/cyclin complexes in transcription and RNA splicing. *Cell. Signalling* **2005**, *17*, 1033–1051.
(7) Wei, F. Y.; Nagashima, K.; Ohshima, T.; Saheki, Y.; Lu, Y. F.; Matsushita, M.; Yamada, Y.; Mikoshiba, K.; Seino, Y.; Matsui, H.; Tomizawa, K. Cdk5-dependent regulation of glucose-stimulated insulin secretion. *Nat. Med.* **2005**, *11*, 1104–1108.
(8) Vermeulen, K.; Van Bockstaele, D. R.; Berneman, Z. N. The cell cycle: a review of regulation, deregulation and therapeutic targets in cancer. *Cell Proliferation* **2003**, *36*, 131–149.
(9) Cruz, J. C.; Tsai, L.-H. Cdk5 deregulation in the pathogenesis of Alzheimer's disease. *Trends Mol. Med.* **2004**, *10*, 452–458.
(10) Smith, P. D.; Crocker, S. J.; Jackson-Lewis, V.; Jordan-Sciutto, K. L.; Hayley, S.; Mount, M. P.; O'Hare, M. J.; Callaghan, S.; Slack, R. S.; Przedborski, S.; Anisman, H.; Park, D. S. Cyclin-dependent kinase 5 is a mediator of dopaminergic neuron loss in a mouse model of Parkinson's disease. *Proc. Natl. Acad. Sci. U.S.A.* **2003**, *100*, 13650–13655.
(11) Smith, P. D.; O'Hare, M. J.; Park, D. S. CDKs: taking on a role as mediators of dopaminergic loss in Parkinson's disease. *Trends Mol. Med.* **2004**, *10*, 445–451.
(12) Zhang, M.; Li, J.; Chakrabarty, P.; Bu, B.; Vincent, I. Cyclin-dependent kinase inhibitors attenuate protein hyperphosphorylation, cytoskeletal lesion formation, and motor defects in Niemann-Pick type C mice. *Am. J. Pathol.* **2004**, *165*, 843–852.
(13) Wang, J.; Liu, S.; Fu, Y.; Wang, J. H.; Lu, Y. Cdk5 activation induces hippocampal CA1 cell death by directly phosphorylating NMDA receptors. *Nat. Neurosci.* **2003**, *6*, 1039–1047.
(14) Rashidian, J.; Iyirhiaro, G.; Aleyasin, H.; Rios, M.; Vincent, I.; Callaghan, S.; Bland, R. J.; Slack, R. S.; During, M. J.; Park, D. S. Multiple cyclin-dependent kinases signals are critical mediators of ischemia/hypoxic neuronal death in vitro and in vivo. *Proc. Natl. Acad. Sci. U.S.A.* **2005**, *102*, 14080–14085.

(15) Di Giovanni, S.; Movsesyan, V.; Ahmed, F.; Cernak, I.; Schinelli, S.; Stoica, B.; Faden, A. I. Cell cycle inhibition provides neuroprotection and reduces glial proliferation and scar formation after traumatic brain injury. *Proc. Natl. Acad. Sci. U.S.A.* **2005**, *102*, 8333–8335.
(16) Schang, L. M. Effects of pharmacological cyclin-dependent kinase inhibitors on viral transcription and replication. *Biochim. Biophys. Acta* **2004**, *1697*, 197–209.
(17) Pumfery, A.; de la Fuente, C.; Berro, R.; Nekhai, S.; Kashanchi, F.; Chao, S. H. Potential use of pharmacological cyclin-dependent kinase inhibitors as anti-HIV therapeutics. *Curr. Pharm. Des.* **2006**, *12*, 1949–1961.
(18) Nelson, P. J.; Shankland, S. J. Therapeutics in renal disease: the road ahead for antiproliferative targets. *Nephron Exp. Nephrol.* **2005**, *103*, e6–e15.
(19) Gherardi, D.; D'Agati, V.; Tearina Hu, T.-H.; Barnett, A.; Gianella-Borradori, A.; Gelman, I. H.; Nelson, P. J. Reversal of collapsing glomerulopathy in mice with the cyclin-dependent kinase inhibitor CYC202. *J. Am. Soc. Nephrol.* **2004**, *15*, 1212–1222.
(20) Griffin, S. V.; Krofft, R. D.; Pippin, J. W.; Shankland, S. J. Limitation of podocyte proliferation improves renal function in experimental crescentic glomerulonephritis. *Kidney Int.* **2005**, *67*, 977–986.
(21) Price, P. M.; Yu, F.; Kaldis, P.; Aleem, E.; Nowak, G.; Safirstein, R. L.; Megeyesi, J. Dependence of cisplatin-induced cell death in vitro and in vivo on cyclin-dependent kinase 2. *J. Am. Soc. Nephrol.* **2006**, *17*, 2434–2442.
(22) Bukanov, N. O.; Smith, L. A.; Klinger, K. W.; Ledbetter, S. R.; Ibraghimov-Beskrovnaya, O. Long-lasting arrest of murine polycystic kidney disease with CDK inhibitor Roscovitine. *Nature* **2006**, *444*, 949–952.
(23) Rossi, A. G.; Sawatzky, D. A.; Walker, A.; Ward, C.; Sheldrake, T. A.; Riley, N. A.; Caldicott, A.; Martinez-Losa, M.; Walker, T. R.; Duffin, R.; Gray, M.; Crescenzi, E.; Martin, M. C.; Brady, H. J.; Savill, J. S.; Dransfield, I.; Haslett, C. Cyclin-dependent kinase inhibitors enhance the resolution of inflammation by promoting inflammatory cell apoptosis. *Nat. Med.* **2006**, *12*, 1056–1064.
(24) Pareek, T. K.; Keller, J.; Kesavapany, S.; Agarwal, N.; Kuner, R.; Pant, H. C.; Iadarola, M. J.; Brady, R. O.; Kulkarni, A. B. Cyclin-dependent kinase 5 modulates nociceptive signaling through direct phosphorylation of transient receptor potential vanilloid 1. *Proc. Natl. Acad. Sci. U.S.A.* **2007**, *104*, 660–665.
(25) Knockaert, M.; Greengard, P.; Meijer, L. Pharmacological inhibitors of cyclin-dependent kinases. *Trends Pharmacol. Sci.* **2002**, *123*, 417–425.
(26) Fischer, P. M.; Gianella-Borradori, A. Recent progress in the discovery and development of cyclin-dependent kinase inhibitors. *Expert Opin. Invest. Drugs* **2005**, *14*, 457–477.
(27) Shapiro, G. I. Cyclin-dependent kinase pathways as targets for cancer treatment. *J. Clin. Oncol.* **2006**, *24*, 1770–1783.
(28) Misra, R. N. Clinical progress of selective cyclin-dependent kinase (CDK) inhibitors. *Drugs Future* **2006**, *31*, 43–52.
(29) *CDK Inhibitors of Cyclin-Dependent Kinases as Anti-Tumor Agents*; Smith, P. J., Yue, E., Eds; Monographs on Enzyme Inhibitors, Vol. 2, CRC Press: Boca Raton, FL, 2006.
(30) Noble, M. E.; Endicott, J. A.; Johnson, L. N. Protein kinase inhibitors: insights into drug design from structure. *Science* **2004**, *303*, 1800–1805.
(31) Bach, S.; Blondel, M.; Meijer, L. Evaluation of CDK Inhibitors' Selectivity: From Affinity Chromatography to Yeast Genetics. In *CDK Inhibitors and Their Potential as Anti-Tumor Agents*; Yue, E, Smith, P. J., Eds; Monographs on Enzyme Inhibitors, Vol. 2; CRC Press: Boca Raton, FL, 2006; pp 103–119.
(32) Gompel, M.; Leost, M.; Bal de Kier Joffe, E.; Puricelli, L.; Hernandez Franco, L.; Palermo, J.; Meijer, L. Meridianins, a new family of protein kinase inhibitors isolated from the Ascidian Aplidium meridianum. *Bioorg. Med. Chem. Lett.* **2004**, *14*, 1703–1707.
(33) Franco, L. H.; Bal de Kier Joffe, E.; Puricelli, L.; Tatian, M.; Seldes, A. M.; Palermo, J. A. Indole alkaloids from the tunicate Aplidium meridianum. *J. Nat. Prod.* **1998**, *61*, 1130–1132.
(34) Fresneda, P. M.; Molina, P.; Delgado, S.; Bleda, J. A. Synthetic studies towards the 2-aminopyrimidine alkaloids variolins and meridianins from marine origin. *Tetrahedron Lett.* **2000**, *41*, 4777–4780.
(35) Jiang, B.; Yang, C.-G. Synthesis of indolylpyrimidines via cross-coupling of indolylboronic acid with chloropyrimidines: facile synthesis of meridianin D. *Heterocycles* **2000**, *53*, 1489–1498.
(36) Franco, L. H.; Palermo, J. A. Synthesis of 2-(pyrimidin-4-yl)indoles. *Chem. Pharm. Bull.* **2003**, *51*, 975–977.
(37) Perry, N. B.; Ettouati, L.; Litaudon, M.; Blunt, J. W.; Munro, M. H. G.; Parkin, S.; Hope, H. Alkaloids from the Antarctic sponge *Kirkpatrickia varialosa*. Part 1: variolin B, a new antitumour and antiviral compound. *Tetrahedron* **1994**, *50*, 3987–3992.
(38) Trimurtulu, G.; Faulkner, D. J.; Perry, N. B.; Ettouati, L.; Litaudon, M.; Blunt, J. W.; Munro, M. H. G.; Jameson, G. B. Alkaloids from the Antarctic sponge *Kirkpatrickia varialosa*. Part 2: variolin A and *N*(3′)-methyltetrahydrovariolin B. *Tetrahedron* **1994**, *50*, 3993–4000.
(39) Anderson, R. J.; Morris, J. C. Total synthesis of variolin B. *Tetrahedron Lett.* **2001**, *42*, 8697–8699.
(40) Molina, P.; Fresneda, P. M.; Delgado, S. Carbodiimide-mediated preparation of the tricyclic pyrido[3′,2′:4,5]pyrrolo[1,2-*c*]pyrimidine ring system and its application to the synthesis of the potent antitumoral marine alkaloid variolin B and analog. *J. Org. Chem.* **2003**, *68*, 489–499.
(41) Ahaidar, A.; Fernandez, D.; Danelon, G.; Cuevas, C.; Manzanares, I.; Albericio, F.; Joule, J. A.; Alvarez, M. Total syntheses of variolin B and deoxyvariolin B. *J. Org. Chem.* **2003**, *68*, 10020–10029.
(42) Mendiola, J.; Baeza, A.; Alvarez-Builla, J.; Vaquero, J. J. Reaction of bromomethylazoles and tosylmethyl isocyanide. A novel heterocyclization method for the synthesis of the core of marine alkaloids variolins and related azolopyrimidines. *J. Org. Chem.* **2004**, *69*, 4974–4983.
(43) Anderson, R. J.; Hill, J. B.; Morris, J. Concise total syntheses of variolin B and deoxyvariolin B. *J. Org. Chem.* **2005**, *70*, 6204–6212.
(44) Erba, E.; Balconi, G.; Faretta, M.; Bergamaschi, D.; Guidi, G.; Jimeno, J.; Faircloth, G.; D'Incalci, M. Cell cycle phase perturbation and apoptosis induced by variolin B, a novel antitumor agent of marine origin. *Proc. Am. Assoc. Cancer Res.* **1996**, *37*, 28.
(45) Simone, M.; Erba, E.; Damia, G.; Vikhanskaya, F.; Di Francesco, A. M.; Riccardi, R.; Bailly, C.; Cuevas, C.; Fernandez Sousa-Faro, J. M.; D'Incalci, M. Variolin B and its derivate deoxy-variolin B: new marine natural compounds with cyclin-dependent kinase inhibitor activity. *Eur. J. Cancer.* **2005**, *41*, 2366–2377.
(46) Fresneda, P. M.; Molina, P.; Bleda, J. A. Synthesis of the indole alkaloids meriadinins from the tunicate aplidium meridianum. *Tetrahedron* **2001**, *57*, 2355–2363.
(47) Girgis, N. S.; Larson, S. B.; Robins, R. K.; Cottam, H. B. The synthesis of 5-azaindoles by substitution-rearrangement of 7-azaindoles upon treatment with certain primary amines. *J. Heterocycl. Chem.* **1989**, *26*, 317–325.
(48) Zhang, Z.; Yang, Z.; Wong, H.; Zhu, J.; Meanwell, N. A.; Kadow, J. F.; Wang, T. An effective procedure for the acylation of azaindoles at C-3. *J. Org. Chem.* **2002**, *67*, 6226–6227.
(49) Kwon, H. B.; McKee, B. H.; Stille, J. K. Palladium-catalyzed coupling reactions of (1-ethoxyvinyl)trimethylstannane with vinyl and aryl triflate. *J. Org. Chem.* **1990**, *55*, 3114–3118.
(50) Helland, I.; Lejon, T. Synthesis of 4-phenylpyrimidine from acetophenone and formamide. *Heterocycles* **1999**, *51*, 611–615.
(51) Fernandez, D.; Ahaidar, A.; Danelon, G.; Cironi, P.; Marfil, M.; Perez, O.; Cuevas, C.; Albericio, F.; Joule, J. A.; Alvarez, M. Synthesis of polyheterocyclic nitrogen-containing marine natural products. *Monatsch. Chem.* **2004**, *135*, 615–627.
(52) Azevedo, W. F.; Leclerc, S.; Meijer, L.; Havlicek, L.; Strnad, M.; Kim, S. H. Inhibition of cyclin-dependent kinases by purine analogues: crystal structure of human cdk2 complexed with roscovitine. *Eur. J. Biochem.* **1997**, *243*, 518–526.
(53) Hoessel, R.; Leclerc, S.; Endicott, J.; Noble, M.; Lawrie, A.; Tunnah, P.; Leost, M.; Damiens, E.; Marie, D.; Marko, D.; Niederberger, E.; Tang, W.; Eisenbrand, G.; Meijer, L. Indirubin, the active constituent of a Chinese antileukaemia medicine, inhibits cyclin-dependent kinases. *Nat. Cell Biol.* **1999**, *1*, 60–67.
(54) Moshinsky, D. J.; Bellamacina, C. R.; Boisvert, D. C.; Huang, P.; Hui, T.; Jancarik, J.; Kim, S. H.; Rice, A. G. SU9516: biochemical analysis of cdk inhibition and crystal structure in complex with cdk2. *Biochem. Biophys. Res. Commun.* **2003**, *310*, 1026–1031.
(55) Davies, T. G.; Bentley, J.; Arris, C. E.; Boyle, F. T.; Curtin, N. J.; Endicott, J. A.; Gibson, A. E.; Golding, B. T.; Griffin, R. J.; Hardcastle, I. R.; Jewsbury, P.; Johnson, L. N.; Mesguiche, V.; Newell, D. R.; Noble, M. E.; Tucker, J. A.; Wang, L.; Whitfield, H. J. Structure-based design of a potent purine-based cyclin-dependent kinase inhibitor. *Nat. Struct. Biol.* **2002**, *9*, 745–749.
(56) Mettey, Y.; Gompel, M.; Thomas, V.; Garnier, M.; Leost, M.; Ceballos-Picot, I.; Noble, M.; Endicott, J.; Vierfond, J.-M.; Meijer, L. Aloïsines, a new family of CDK/GSK-3 inhibitors. SAR study, crystal structure in complex with CDK2, enzyme selectivity, and cellular effects. *J. Med. Chem.* **2003**, *46*, 222–236.
(57) Leclerc, S.; Garnier, M.; Hoessel, R.; Marko, D.; Bibb, J. A.; Snyder, G. L.; Greengard, P.; Biernat, J.; Mandelkow, E.-M.; Eisenbrand, G.; Meijer, L. Indirubins inhibit glycogen synthase kinase-3β and CDK5/p25, two kinases involved in abnormal tau phosphorylation in Alzheimer's disease. A property common to most CDK inhibitors? *J. Biol. Chem.* **2001**, *276*, 251–260.
(58) Huang, S.; Li, R.; Connolly, P. J.; Emanuel, S.; Middleton, S. A. Synthesis of 2-amino-4-(7-azaindol-3-yl)pyrimidines as cyclin dependent kinase 1 (CDK1) inhibitors. *Bioorg. Med. Chem. Lett.* **2006**, *16*, 4818–4821.
(59) Zarkowska, T.; Mittnacht, S. Differential phosphorylation of the retinoblastoma protein by G1/S cyclin-dependent kinases. *J. Biol. Chem.* **1997**, *272*, 12738–12746.

(60) Kwon, Y. G.; Lee, S. Y.; Choi, Y.; Greengard, P.; Nairn, A. C. Cell cycle-dependent phosphorylation of mammalian protein phosphatase 1 by cdc2 kinase. *Proc. Natl. Acad. Sci. U.S.A.* **1997**, *94*, 2168–2173.
(61) Ahn, S. H.; Kim, M.; Buratowski, S. Phosphorylation of serine 2 within the RNA polymerase II C-terminal domain couples transcription and 3′ end processing. *Mol. Cell* **2004**, *13*, 67–76.
(62) Mandelin, A. M.; Pope, R. M. Myeloid cell leukemia-1 as a therapeutic target. *Expert Opin. Ther. Targets* **2007**, *11*, 363–373.
(63) Yang-Yen, H. F. Mcl-1: a highly regulated cell death and survival controller. *J. Biomed. Sci.* **2006**, *13*, 201–204.
(64) Del Duca, D.; Werbowetski, T.; Del Maestro, R. F. Spheroid preparation from hanging drops: characterization of a model of brain tumor invasion. *J. Neurooncol.* **2004**, *67*, 295–303.
(65) Desosize, D.; Jardillier, J. Multicellular resistance: a paradigm for clinical resistance. *Crit. Rev. Oncol. Hematol.* **2000**, *36*, 193–207.
(66) Bettayeb, K.; Tirado, O. M.; Marionneau-Lambert, S.; Ferandin, Y.; Lozach, O.; Morris, J.; Mateo-Lozano, S.; Drückes, P.; Schächtele, C.; Kubbutat, M.; Liger, F.; Marquet, B.; Joseph, B.; Echalier, A.; Endicott, J.; Notario, V.; Meijer, L. Meriolins, a new class of cell death-inducing kinase inhibitors with inhibitors with enhanced selectivity for cyclin-dependent kinases. *Cancer Res.* **2007**, *67*, 8325–8334.
(67) Brown, N. R.; Noble, M. E.; Endicott, J. A.; Johnson, L. N. The structural basis for specificity of substrate and recruitment peptides for cyclin-dependent kinases. *Nat. Cell Biol.* **1999**, *1*, 438–443.
(68) Collaborative Computational Project, Number 4. The CCP4 suite: programs for protein crystallography. *Acta Crystallogr.* **1994**, *D50*, 760–763.
(69) Emsley, P.; Cowtan, K. Coot: model-building tools for molecular graphics. *Acta Crystallogr.* **2004**, *D60*, 2126–2132.
(70) Murshudov, G. N.; Vagin, A. A.; Dodson, E. J. Refinement of macromolecular structures by the maximum-likelihood method. *Acta Crystallogr.* **1997**, *D53*, 240–255.
(71) Marin, O.; Meggio, F.; Pinna, L. A. Design and synthesis of two new peptide substrates for the specific and sensitive monitoring of casein kinases 1 and 2. *Biochem. Biophys. Res. Commun.* **1984**, *198*, 898–905.
(72) Meijer, L.; Borgne, A.; Mulner, O.; Chong, J. P. J.; Blow, J. J.; Inagaki, N.; Inagaki, M.; Delcros, J. G.; Moulinoux, J. P. Biochemical and cellular effects of roscovitine, a potent and selective inhibitor of the cyclin-dependent kinases cdc2, cdk2 and cdk5. *Eur. J. Biochem.* **1997**, *243*, 527–536.
(73) Primot, A.; Baratte, B.; Gompel, M.; Borgne, A.; Liabeuf, S.; Romette, J. L.; Costantini, F.; Meijer, L. Purification of GSK-3 by affinity chromatography on immobilised axin. *Protein Expression Purif.* **2000**, *20*, 394–404.
(74) Reinhardt, J.; Ferandin, Y.; Meijer, L. Purification of native, active casein kinase 1 (CK1) by affinity chromatography on immobilised axin fragment. *Protein Expression Purif.* **2007**, *54*, 101–109.
(75) Namba, M.; Ohtsuki, T.; Mori, M.; Togawa, A.; Wada, H.; Sugihara, T.; Yawata, Y.; Kimoto, T. Establishment of five human myeloma cell lines. *In Vitro Cell Dev. Biol.* **1989**, *25*, 723–729.
(76) Cartron, P.-F.; Juin, P.; Oliver, L.; Martin, S.; Meflah, K.; Vallette, F. M. Nonredundant role of Bax and Bak in Bid-mediated apoptosis. *Mol. Cell. Biol.* **2003**, *23*, 4701–4712.
(77) Ribas, J.; Boix, J. Cell differentiation, caspase inhibition, and macromolecular synthesis blockage, but not BCL-2 or BCL-XL proteins, protect SH-SY5Y cells from apoptosis triggered by two CDK inhibitory drugs. *Exp. Cell Res.* **2004**, *295*, 9–24.
(78) Christian, B. A.; Grever, M. R.; Byrd, J. C.; Lin, T. S. Flavopiridol in the treatment of chronic lymphocytic leukemia. *Curr. Opin. Oncol.* **2007**, *19*, 573–578.
(79) Meijer, L.; Raymond, E. Roscovitine and other purines as kinase inhibitors. From starfish oocytes to clinical trials. *Acc. Chem. Res.* **2003**, *36*, 417–25.
(80) Meijer, L.; Bettayeb, K.; Galons, H. Roscovitine (CYC202, Seliciclib). In *CDK Inhibitors and Their Potential as Anti-Tumor Agents*; Yue, E., Smith, P. J., Eds.; Monographs on Enzyme Inhibitor, Vol. 2; CRC Press: Boca Raton, FL, 2006; pp 187–226.
(81) Chu, X. J.; DePinto, W.; Bartkovitz, D.; So, S.-S.; Vu, B. T.; Packman, K.; Lukacs, C.; Ding, Q.; Jiang, N.; Wang, K.; Goelzer, P.; Yin, X.; Smith, M. A.; Higgins, B. X.; Chen, Y.; Xiang, Q.; Moliterni, J.; Kaplan, G.; Graves, B.; Lovey, A.; Fotouhi, N. Discovery of [4-amino-2-(1-methanesulfonylpiperidin-4-ylamino)pyrimidin-5-yl](2,3-difluoro-6-methoxyphenyl)methanone (R547), a potent and selective cyclin-dependent kinase inhibitor with significant in vivo antitumor activity. *J. Med. Chem.* **2006**, *49*, 6549–6560.
(82) DePinto, W.; Chu, X.-J.; Yin, X.; Smith, M.; Packman, K.; Goelzer, P.; Lovey, A.; Chen, Y.; Qian, H.; Hamid, R.; Xiang, Q.; Tovar, C.; Blain, R.; Nevins, T.; Higgins, B.; Luistro, L.; Kolinsky, K.; Felix, B.; Hussain, S.; Heimbrook, D. In vitro and in vivo activity of R547: a potent and selective cyclin-dependent kinase inhibitor currently in phase I clinical trials. *Mol. Cancer Ther.* **2006**, *5*, 2644–2658.
(83) Misra, R. N.; Xiao, H.-Y.; Kim, K. S.; Lu, S.; Han, W.-C.; Barbosa, S. A.; Hunt, J. T.; Rawlins, D. B.; Shan, W.; Ahmed, S. Z.; Qian, L.; Chen, B.-C.; Zhao, R.; Bednarz, M. S.; Kellar, K. A.; Mulheron, J. G.; Batorsky, R.; Roongta, U.; Kamath, A.; Marathe, P.; Ranadive, S. A.; Sack, J. S.; Tokarski, J. S.; Pavletich, N. P.; Lee, F. Y. F.; Webster, K. R.; Kimball, S. D. *N*-(Cycloalkylamino)acyl-2-aminothiazole inhibitors of cyclin-dependent kinase 2. *N*-[5-[[[5-(1,1-Dimethylethyl)-2-oxazolyl]methyl]thio]-2-thiazolyl]-4-piperidinecarboxamide (BMS-387032), a highly efficacious and selective antitumor agent. *J. Med. Chem.* **2004**, *47*, 1719–1728.
(84) Baughn, L. B.; Di Liberto, M.; Wu, K.; Toogood, P. L.; Louie, T.; Gottschalk, R.; Niesvizky, R.; Cho, H.; Ely, S.; Moore, M. A. S.; Chen-Kiang, S. A novel orally active small molecule potently induces G1 arrest in primary myeloma cells and prevents tumor growth by specific inhibition of cyclin-dependent kinase 4/6. *Cancer Res.* **2006**, *66*, 7661–7667.
(85) Camidge, D. R.; Smethurst, D.; Growcott, J.; Barrass, N. C.; Foster, J. R.; Febbraro, S.; Swaisland, H.; Hughes, A. A first-in-man phase I tolerability and pharmacokinetic study of the cyclin-dependent kinase-inhibitor AZD5438 in healthy male volunteers. *Cancer Chemother. Pharmacol.* **2007**, *60*, 391–398.
(86) Davies, T. G.; Tunnah, P.; Meijer, L.; Marko, D.; Eisenbrand, G.; Endicott, J. A.; Noble, M. Inhibitor binding to active and inactive CDK2. The crystal structure of CDK2-cyclin-A/indirubin-5-sulphonate. *Structure* **2001**, *9*, 389–397.
(87) Davies, T. G.; Pratt, D. J.; Endicott, J. A.; Johnson, L. N.; Noble, M. E. M. Structure-based design of cyclin-dependent kinase inhibitors. *Pharmacol. Ther.* **2002**, *93*, 125–133.
(88) Kontopidis, G.; McInnes, C.; Pandalaneni, S. R.; McNae, I.; Gibson, D.; Mezna, M.; Thomas, M.; Wood, G.; Wang, S.; Walkinshaw, M.; Fischer, P. M. Differential binding of inhibitors to active and inactive CDK2 provides insights for drug design. *Chem. Biol.* **2006**, *13*, 201–211.

JM700940H

Supporting Information

Meriolins (3-(pyrimidin-4-yl)-7-azaindoles): synthesis, kinase inhibitory activity, cellular effects and structure of a CDK2/cyclin A/meriolin complex

Aude **ECHALIER**, Karima **BETTAYEB**, Yoan **FERANDIN**, Olivier **LOZACH**, Monique **CLEMENT**, Annie **VALETTE**, François **LIGER**, Bernard **MARQUET**, Jonathan C. **MORRIS**, Jane A. **ENDICOTT** , Benoît **JOSEPH** and Laurent **MEIJER**

Elemental analyses

Compounds	Calculated	Found
2d	C: 66.65; H: 6.21; N: 17.27	C: 66.32; H: 6.29; N: 17.39
2e	C: 68.16; H: 6.86; N: 15.90	C: 67.89; H: 6.72; N: 16.01
2f	C: 68.16; H: 6.86; N: 15.90	C: 68.18; H: 6.92; N: 16.02
3a	C: 55.54; H: 3.63; N: 14.39	C: 55.16; H: 3.55; N: 14.28
3b	C: 63.15; H: 5.30; N: 14.73	C: 63.39; H: 5.27; N: 14.80
3c	C: 45.22; H: 2.95; N: 11.72	C: 44.84; H: 3.05; N: 11.90
3d	C: 64.69; H: 5.92; N: 13.72	C: 65.03; H: 6.17; N: 13.86
3e	C: 66.04; H: 6.47; N: 12.84	C: 65.78; H: 6.40; N: 13.01
4a	C: 53.82; H: 3.31; N: 8.37	C: 54.17; H: 3.42; N: 8.55
4b	C: 58.17; H: 4.27; N: 8.48	C: 58.34; H: 4.33; N: 8.60
4c	C: 47.51; H: 2.92; N: 7.39	C: 47.44; H: 3.10; N: 7.40
4d	C: 59.29; H: 4.68; N: 8.13	C: 59.19; H: 4.60; N: 7.96
4e	C: 60.32; H: 5.06; N: 7.82	C: 60.02; H: 4.97; N: 7.67
5	C: 39.76; H: 3.67; N: 9.27	C: 40.10; H: 3.83; N: 9.39
6	C: 43.45; H: 3.42; N: 6.33	C: 43.44; H: 3.45; N: 6.28
4f	C: 60.32; H: 5.06; N: 7.82	C: 60.66; H: 5.15; N: 7.99

4g	C: 64.69; H: 5.92; N: 13.72	C: 64.75; H: 6.01; N: 13.66
7a	C: 55.46; H: 4.14; N: 10.78	C: 55.55; H: 4.14; N: 10.83
7b	C: 59.21; H: 4.97; N: 10.90	C: 59.55; H: 5.08; N: 11.04
7c	C: 49.78; H: 3.71; N: 9.68	C: 49.88; H: 3.71; N: 9.60
7d	C: 60.14; H: 5.30; N: 10.52	C: 59.86; H: 5.42; N: 10.47
7e	C: 61.00; H: 5.61; N: 10.16	C: 60.83; H: 5.53; N: 10.02
7f	C: 61.00; H: 5.61; N: 10.16	C: 60.74; H: 5.80; N: 10.33
7g	C: 64.85; H: 6.61; N: 16.20	C: 64.94; H: 6.75; N: 16.32
1a	C: 53.78; H: 3.28; N: 28.51	C: 53.99; H: 3.35; N: 28.46
1b	C: 59.74; H: 4.60; N: 29.03	C: 59.97; H: 4.51; N: 29.14
1c	C: 45.54; H: 2.78; N: 24.14	C: 45.50; H: 2.76; N: 24.00
1d	C: 61.17; H: 5.13; N: 27.43	C: 61.51; H: 5.32; N: 27.61
1e	C: 62.44; H: 5.61; N: 26.00	C: 62.32; H: 5.70; N: 25.84
1f	C: 62.44; H: 5.61; N: 26.00	C: 62.55; H: 5.47; N: 25.85
1g	C: 61.17; H: 5.13; N: 27.43	C: 61.43; H: 5.27; N: 27.64
1h	C: 58.94; H: 5.30; N: 24.55	C: 59.33; H: 5.51; N: 24.66
8	C: 58.15; H: 3.99; N: 30.82	C: 58.00; H: 4.11; N: 30.88
9	C: 59.74; H: 4.60; N: 29.03	C: 60.02; H: 4.74; N: 28.99
10	C: 63.71; H: 4.46; N: 24.76	C: 63.59; H: 4.53; N: 24.86
11	C: 62.26; H: 3.80; N: 26.40	C: 62.00; H: 3.85; N: 26.23
12	C: 57.34; H: 4.44; N: 20.57	C: 56.97; H: 4.23; N: 20.44

Comparison of meriolin 5 (1e) with other CDK inhibitors

Roscovitine (Fig. 5B)

The structure of monomeric (inactive) CDK2 in complex with roscovitine has been reported [52]. However, because activation of CDK2 by association with cyclin A/E and by phosphorylation triggers dramatic conformational changes within the CDK2 fold, we decided to determine the structure of the fully activated CDK2 (pThr160-CDK2/cyclin A) in complex with roscovitine (our unpublished results). Roscovitine binding to the CDK2 ATP site shares features with meriolin 5. Briefly, the central scaffolds of these two inhibitors, the pyrrolo-pyridine in meriolin and the purine in roscovitine, occupy similar positions in the ATP cleft. There is a slight twist of the roscovitine scaffold towards CDK2 hinge and pendant groups in each inhibitor explore different regions of the ATP binding site (Fig. 5B). Meriolin 5 mainly probes the hydrophobic region to the left of the gatekeeper residue, Phe80. Roscovitine however explores the specificity surface outside the ATP binding site and the region underneath the CDK2 glycine-rich loop. Roscovitine binding to CDK2 is accompanied by the presence of ordered water molecules at the entrance of the ATP binding site. Both meriolin 5 and roscovitine make hydrophobic interactions with the apolar side chains of Leu134 and Ala31 and in addition the Ile10 side chain interacts with the roscovitine purine ring. Other hydrophobic interactions stabilise roscovitine within the CDK2 ATP binding site. The isopropyl group packs against the gatekeeper residue and is in close contact with the side chain of Val64 and the methyl group of the aminobutanol moiety contacts main chain atoms of Gln131 and Asn132. It is not clear if these contacts are favourable to roscovitine binding.

Roscovitine makes hydrogen bonds with CDK2 hinge region via one nitrogen of the purine ring to the Leu83 main chain amide nitrogen and one amine group of the phenylmethanamine group to the Leu83 main chain carbonyl moiety. Consequently the phenylmethanamine group of roscovitine binds to the specificity surface on the C-terminal domain outside the CDK2 active site. There are also differences between the roscovitine and meriolin5 binding sites. In the meriolin structure, the pyrrole ring directly faces the gatekeeper, Phe80 whereas this region is occupied by an isopropyl group in the roscovitine bound structure. The imidazole group of the purine ring is also slightly turned

towards the hinge region in comparison with its counterpart in meriolin 5, the pyrrole group. The hydrophobic pocket at the back of the ATP binding cleft is not fully occupied by roscovitine (one methyl group from the isopropyl) in contrast with the meriolin 5-bound structure in which it is filled by the pyrimidin-amine group. The aminobutanol group of roscovitine packs against the glycine-rich loop whereas meriolin 5 does not probe this region extensively.

Oxindoles (indirubin-3'-oxime-5-sulphonate and SU9516) (Fig. 5C, 5D)

The central scaffolds of meriolin 5 (pyrrolo-pyridine) and of the two oxindole representatives, indirubin-3'-oxime-5-sulphonate and SU9516 (indoline) occupy a very different position within the CDK2 ATP binding site. While as described previously the pyrrole group of meriolin 5 faces Phe80 it is the benzene ring of indirubin-3'-oxime-5-sulphonate and the SU9516 indoline ring that packs against the aromatic side chain of Phe80. In contrast to meriolin 5, the oxindole inhibitors make three hydrogen bonds with the CDK2 hinge region. Additionally the sulphonate moiety of indirubin-3'-oxime-5-sulphonate is engaged in complementary charge interactions with the side chain of Lys33 and the Asp145 main chain amide nitrogen. The position of the sulphonate moiety is reminiscent of that of the ATP α- phosphate. The reason for the different position of the pyrrole ring and the indoline ring in the ATP cleft probably results from the lack of a hydrogen bond acceptor on the indoline benzene ring (which prevents formation of the typical hydrogen bond with the hinge region in the pyrrole 'orientation') and from the presence of the ketone group on the indoline scaffold which could generate a steric clash with the Phe80 side chain in the 'pyrrole orientation' of meriolin 5.

The very extended ring system of indirubin-3'-oxime-5-sulphonate results in several hydrophobic contacts with the side chains of Leu134, Ala31 and Ile10 as well as favourable packing of the inhibitor against the gatekeeper side chain.

NU2058 (Fig. 5E)

The binding mode of NU2058 ((6-cyclohexylmethoxy)-9*H*-purin-2-amine) to CDK2 is reminiscent of that of meriolin 5 in that the pyrrolo-pyridine ring of meriolin 5 and the NU2058 purine ring occupy almost identical locations within the active site. However, the meriolin 5 pyrrole ring penetrates slightly further (0.6 Å) towards the

gatekeeper. This probably results from the hydrogen bonds between the meriolin 5 pyrimidine-amine group with the side chains of Glu51 and Lys33 that stabilise the inhibitor deeper within the cleft, whereas NU2058 forms an additional hydrogen bond with the more distant part of the CDK2 hinge at Leu83. This additional hydrogen bond was shown in the NU series to confer increased inhibitory activity. The presence of this amine group on the pyrimidine ring of NU2058 and the formation of the hydrogen bond between this amine and the hinge region are probably responsible for a small conformational change in the hinge region at Leu83-His84. A similar movement of the hinge region away from the ATP binding site is also observed in complexes of CDK2 with SU9516 (3-((1*H*-imidazol-5-yl)methyl)-5-methoxyindolin-2-one) and to a lesser extent with indirubin-3'-oxime-5-sulphonate.

Finally, interactions with the glycine-rich loop are explored by the roscovitine aminobutanol group, by the NU2058 cyclohexyl group and by the meriolin 5 propoxy group.

Aloisine A (Fig. 5F)

The binding mode of aloisine A is relatively similar to that of variolin B, in that the presence of the phenol group in aloisine A results in the pyrrole group of the pyrrolo-pyrazine scaffold facing towards the outside of the active site. Additionally the absence of a hydrogen bond donor on the pyrazine ring results in a displacement of the inhibitor along the hinge region. This displacement allows the formation of two hydrogen bonds with the main chain amide and carbonyl groups of Leu83. As observed in the structure of roscovitine bound to CDK2, the aloisine A phenol group probes the selectivity surface contributed by the CDK2 C-terminal domain. The isopropyl moiety of aloisine A occupies a similar position within the ribose binding site as the meriolin 5 propanol group.

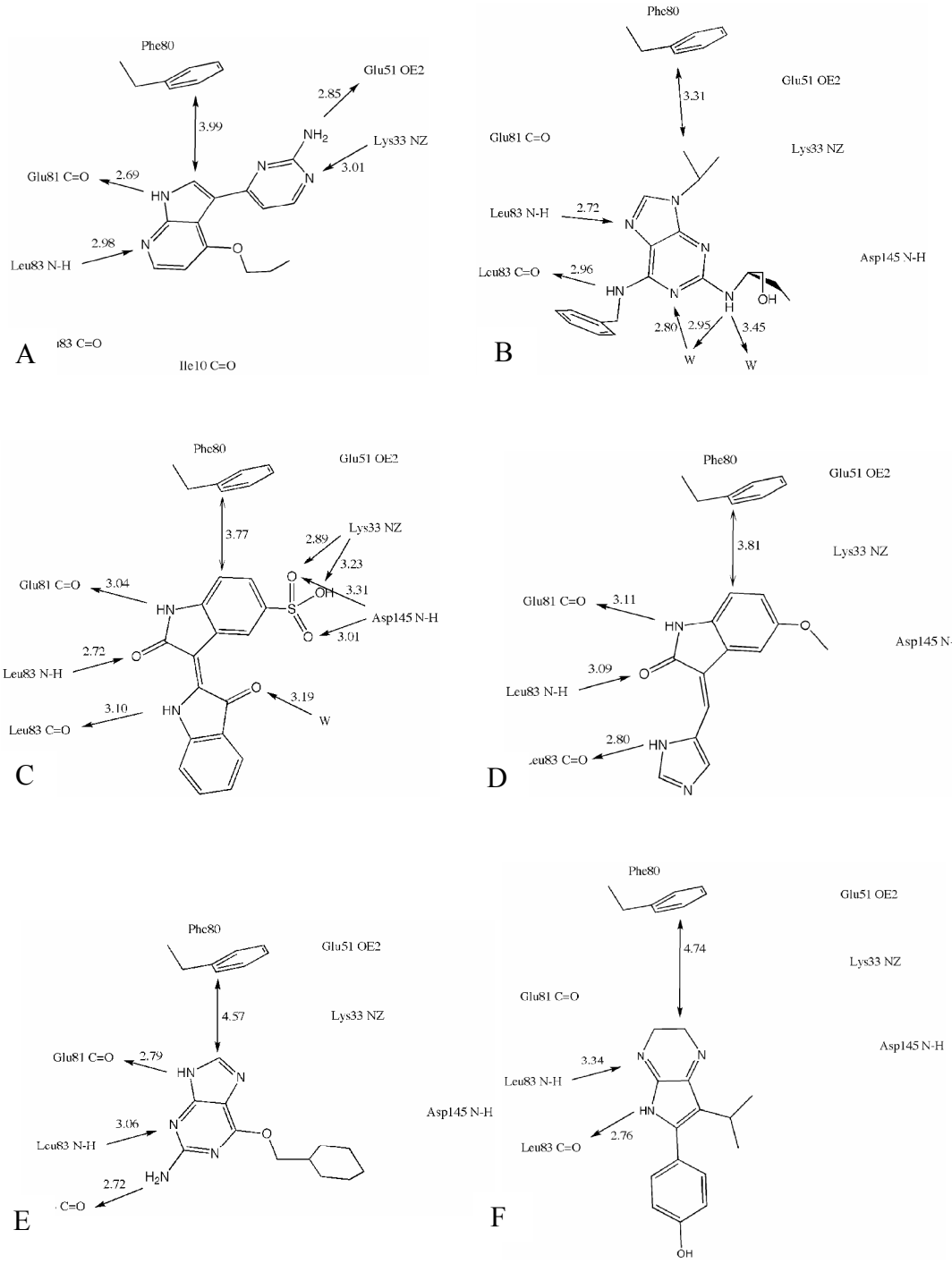

Figure S5: Comparative diagram of the binding modes of meriolin 5 and other protein kinase inhibitors. Panels correspond to meriolin 3 (A), roscovitine (B), indirubin-3'-oxime-5-sulphonate (C), SU9516 (D), NU2058 (E), aloisine A (F) bound to CDK2. All the inhibitors presented in this figure are bound to the active form of CDK2 in complex with cyclin A with the exception of SU9516 that is bound to monomeric inactive CDK2.